Original Article

Lipids in xylem sap of woody plants across the angiosperm phylogeny

H. Jochen Schenk[1,*], Joseph M. Michaud[1], Susana Espino[1], Tatiana Melendres[1], Mary R. Roth[2], Ruth Welti[2], Lucian Kaack[3], and Steven Jansen[3]

[1]Department of Biological Science, California State University Fullerton, 800 N. State College Boulevard, Fullerton, CA 92831, USA; [2]Kansas Lipidomics Research Center; Division of Biology; Kansas State University; Manhattan, KS 66506, USA; [3]Institute of Systematic Botany and Ecology, Ulm University, Albert-Einstein-Allee 11, D–89081, Ulm, Germany.

[*]For correspondence. E-mail jschenk@fullerton.edu

Short-running title: Lipids in angiosperm xylem

Keywords: angiosperms, apoplast, cohesion-tension theory, galactolipids, lipidomics, phospholipids, vessel volume, xylem, xylem sap, *Laurus nobilis*

Lipids have been observed attached to lumen-facing surfaces of mature xylem conduits of several plant species, but there has been no research on their functions or effects on water transport, and only one lipidomic study of the xylem apoplast. Therefore, we conducted lipidomic analyses of xylem sap from seven plants representing six major angiosperm clades, including basal angiosperms, monocots, and eudicots, to characterize and quantify phospholipids, galactolipids, and sulfolipids in sap. We also imaged locations of lipids in vessels of *Laurus nobilis* using confocal and transmission electron microscopy (TEM). Xylem sap was extracted from cut woody stems, partially freeze-dried to concentrate the sap, extracted, and analyzed via mass spectrometry. Lipids were imaged in xylem using TEM and confocal microscopy. Lipids in xylem sap included the galactolipids di- and mono-galactosyldiacylglycerol (DGDG and MGDG), as well as all common plant phospholipids, but only traces of sulfolipids, with total lipid concentrations ranging from 0.18 to 0.63 μmol / L across all seven species. Lipid layers coated all lumen-facing vessel surfaces of *Laurus nobilis*, and lipids were highly concentrated in inter-vessel pits. The findings suggest that apoplastic, amphiphilic xylem lipids are a universal feature of angiosperms. They are concentrated in inter-vessel pits, where their low surface tension is likely to affect bubble entry via air seeding from gas-filled conduits. The findings force a reinterpretation of the cohesion-tension theory of water transport to account for the effects of apoplastic lipids on the dynamic surface tension in the xylem and on hydraulic conductance through inter-vessel pits.

INTRODUCTION

The lipidome of the plant apoplast has been characterized as a black box (Misra, 2016), because there have been almost no lipidomic analyses of cell walls, intercellular spaces, and xylem conduits and fibers, except for a few studies of surface lipids involved in the making of suberin, cutin, and waxes. Studies of lipids in xylem conduits are especially limited. Wagner et al. (2000) observed under transmission electron microscopy (TEM) a dark layer lining xylem conduit surfaces of the resurrection plant *Myrothamnus flabellifolia* Welw. (Myrothamnaceae) and after further studies concluded that it was composed of phospholipids (Schneider et al., 2003). Dark layers on vessel walls that appeared under TEM after OsO_4 fixation were also found in a few other species (Fineran, 1997, Zimmermann et al., 2004, Westhoff et al., 2008). In fact, it had been suggested much earlier that a thin coat of lipids may remain on the lumen walls of conduits from live cell content after conduit maturation (Scott et al., 1960, Esau, 1965, Esau et al., 1966).

The presence of lipids in xylem conduits may seem difficult to reconcile with the cohesion tension (CT) theory of water transport (Askenasy, 1895, Dixon and Joly, 1895), which posits the existence of negative pressure (i.e., tension) in xylem sap. Lipids are either hydrophobic or amphiphilic, either of which properties would appear to pose a problem for maintaining negative pressure in the sap without forming gas bubbles on hydrophobic or amphiphilic surfaces. Accordingly, Zimmermann et al. (2004) cited evidence for lipids in the xylem apoplast to bolster their arguments against the CT theory. However, the CT theory is strongly supported by multiple lines of evidence, both indirect and direct (Angeles et al., 2004, Wheeler and Stroock, 2008, Jansen and Schenk, 2015, Venturas et al., 2017), so the existence of apoplastic xylem lipids would require an explanation within the context of this theory (Schenk et al., 2017).

Any idea that there are no amphiphilic lipids in the xylem apoplast was put to rest when Gonorazky et al. (2012) published an analysis of phospholipids in intercellular fluids and xylem fluids of tomato plants. This was followed by reports of phospholipids in xylem sap and on conduit surfaces of five woody angiosperm species from diverse phylogenetic backgrounds

SUBMITTED MANUSCRIPT

(Schenk et al., 2017, Schenk et al., 2018). These findings raise questions about the origins of these lipids, which could be remains from previous living cell content (Scott et al., 1960; Esau, 1965; Esau et al., 1966b) or potentially be transported into vessels from conduit-associated parenchyma cells (Morris et al., 2018b). Even more important are questions about their functions in xylem (Schenk et al., 2015, Schenk et al., 2017). However, surely the first question about these lipids regards their chemical nature. What are they? There is clear evidence for phospholipids in the xylem apoplast, but what are their characteristics and how about galacto- and sulfolipids? To answer these questions, we conducted a lipidomic analysis of xylem sap extracted from seven species sampled across the angiosperm phylogeny, including five woody angiosperm species included in previous studies (Schenk et al., 2017, Schenk et al., 2018), to quantify and characterize all phospho- and galactolipids in xylem sap and test for the presence of sulfolipids in a subset of species. In addition, locations of lipids in xylem were visualized via confocal and transmission electron microscopy in bay laurel, *Laurus nobilis*, a species much studied for its hydraulic properties (e.g., Tyree et al., 1999, Zwieniecki et al., 2001, Hacke and Sperry, 2003, Gascó et al., 2006, Espino and Schenk, 2011, Nardini et al., 2017).

MATERIAL AND METHODS

Plant species

The study was conducted with seven plant species from six major angiosperm clades (APG III, 2009) and different growth forms: *Liriodendron tulipifera* L. (winter-deciduous tree, Magnoliaceae, Magnoliales, magnoliid clade), *Laurus nobilis* L., (evergreen tree, Lauraceae, Laurales, magnoliid clade), *Bambusa oldhamii* Munro (bamboo, Poaceae, Poales, commelinid clade), *Triadica sebifera* Small (syn. *Sapium sebiferum*, winter-deciduous tree, Euphorbiaceae, Malpighiales, fabid clade), *Geijera parviflora* Lindl. (evergreen tree, Rutaceae, Sapindales, malvid clade), *Distictis buccinatoria* (DC.) A.H.Gentry (evergreen liana, Bignoniaceae,

Lamiales, lamiid clade), and *Encelia farinosa* Torr. & A.Gray (drought-deciduous desert shrub, Asteraceae, Asterales, campanulid clade). All grow in the Fullerton Arboretum or on the California State University Fullerton campus in Fullerton, California, United States, except for *Laurus nobilis*, which was collected from the Los Angeles County Arboretum in Arcadia, California, United States. Specimens of *Laurus nobilis* for imaging studies were collected from the Botanical Garden at Ulm University, Germany. All species will be referred to by their genus names in this paper.

Xylem sap extraction

Stems for xylem sap extraction were collected in August 2017 from *Liriodendron*, *Triadica*, *Geijera*, *Distictis*, and *Encelia* and in May 2018 from *Bambusa* and *Laurus*. Most collections were done at dawn to ensure full hydration of stems. The previously published method for xylem sap extraction (Schenk et al., 2017) was modified to completely eliminate contact of xylem sap with hydrophobic surfaces in order to avoid loss of lipids that could cling to such surfaces. Samples were only in contact with glass or with LoBind surfaces of microcentrifuge tubes (Eppendorf AG, Hamburg Germany), which consist of a two-component polymer mix that creates a hydrophilic surface. Branches were cut from the plants at a length exceeding the longest vessel for each species, which had been previously measured via air injection (Greenidge, 1952). Stems were transported immediately to the lab, and cut under water, with the final cuts made with a fresh razor blade. The bark was removed from the proximal end for about 4 cm length to expose the xylem cylinder. The cut surface was thoroughly cleaned with deionized water using a high-pressure dental flosser (WP-100 Ultra Water Flosser, Waterpik Inc., Fort Collins, CO, USA) for two minutes to remove cell debris and cytoplasmic content from the surface. A control sample to determine the amount of contamination from living cell remnants from the cleaned, cut surface was taken by inserting the cut end into a glass vial containing 1 mL of nanopure water and leaving it there for one minute. The liquid was then moved in a glass pipette into a pre-weighed 1.5 mL LoBind Eppendorf microcentrifuge tube, immediately flash-frozen in liquid nitrogen, and stored in the freezer until further processing.

Xylem sap was extracted under vacuum. Tight-fitting latex tubing, about 2 cm long, was fitted over about half of the exposed xylem cylinder next to the bark, leaving about 2 cm of xylem

SUBMITTED MANUSCRIPT

cylinder freely exposed. The stem was then inserted from the top into a rubber flanged stopper, avoiding any contact of the xylem with the stopper during insertion and creating a tight seal between latex tubing and the stopper. The exposed xylem cylinder was then cleaned again with deionized water using a high-pressure dental flosser and excess water removed with a Kimwipe. Xylem sap was collected in a glass test tube embedded in ice inside a 1 L Buchner flask, which was also embedded in ice. The flask was subjected to lab vacuum for about 30 seconds. The distal end of the branch was then cut back by about 4 cm, followed by successive 2 cm cuts, which were made to all the side branches of the stem until sap was observed dripping into the test tube. Once dripping sap was observed, further 1 cm cuts were made every minute to allow for slow, continuous removal of xylem sap. Depending on stem size, 1 to 2 mL of sap were extracted from each stem, moved in a glass pipette into pre-weighed 1.5 mL LoBind Eppendorf microcentrifuge tubes, flash-frozen in liquid nitrogen and stored in the freezer until further processing.

In preliminary experiments we had found that lipid extraction from completely freeze-dried sap samples was incomplete, most likely due to formation of insoluble aggregates. We therefore developed a new protocol to partially freeze-dry samples for lipid extraction and thereby avoid aggregate formation, which yielded about 8 times more lipids than complete freeze-drying (data not shown). For this protocol, weighed cell contamination controls and xylem sap samples of about 1 mL in pre-weighed LoBind Eppendorf microcentrifuge tunes were partially lyophilized in a freeze-dryer (FreeZone 1 Liter Benchtop Freeze Dry System, Labconco, Kansas City, MO, USA) and observed until only about 100 µL of sample remained. They were then taken from the freeze-dryer and weighed again to determine the remaining volume of aqueous sample. The remaining aqueous samples in two (for *Encelia*, *Bambusa*, and *Laurus* xylem sap and *Bambusa* and *Laurus* controls) or four (all xylem sap and controls from all other species) LoBind microcentrifuge tubes were combined into one sample originating from 2 mL or 4 mL (see breakdown of species and controls above) of xylem sap or control using a glass pipette. Methanol:chloroform 1:1 (both HPLC grader, Fisher Scientific) was added to the combined aqueous sample to create an approximate 5:5:1 methanol:chloroform:water one-phase mixture. The mixture was then vortexed, centrifuged, and the supernatant collected with a 1 mL glass syringe with PrecisionGlide Needle. A new one-phase 5:5:1 mixture of methanol:chloroform:water was then added to the residue, the mixture vortexed, centrifuged, and

SUBMITTED MANUSCRIPT

the supernatant again collected and combined with the previously collected supernatant. Samples were then dried in a desiccator outfitted with an in-line carbon filter capsule (model 6704-7500, Whatman, GE Healthcare Life Sciences, UK) and sent to the Kansas Lipidomics Research Center at Kansas State University for mass spectrometry analysis.

Vessel volume analysis

Because lipid micelles are mostly too large to pass through pit membranes, it was hypothesized that lipid concentrations in extracted xylem sap would be related to the volume of vessels opened when a stem is cut for sap extraction. To determine the average opened vessel volume for each species, we used silicone injections (Sperry et al., 2005, Wheeler et al., 2005). Silicone compound (Rhodorsil RTV-141; Rhodia USA, Cranbury, NJ, USA) mixed with 0.41% blue silicone dye (Blue Silc Pig; Smooth On, Easton, PA, USA) was injected from the proximal end into flushed stems (n = 4 per species) that were between 0.9 and 1.7 cm in diameter and 25 cm in length, except 50 cm in length for *Distictis*. Injection took place at approximately 50 kPa for 24 hours, after which the silicone was allowed to dry for 72 hours prior to sectioning. Cross sections (cut at 0.7, 1.4, 2.9, 5.8, 8.3, 11.8, and 24 cm from the cut surface for all species, except at 0.7, 1.4, 2.8, 5.8, 11.6, 16.6, 23.6, and 48 cm for *Distictis*) were thin-sectioned using a sledge microtome (model GSL 1, Schweingruber, Switzerland), dry-mounted on glass slides, and imaged using a Leica MZ16 stereomicroscope with digital camera (model INFINITY 2-1C-IQ, Lumenera, Ottawa, ONT, Canada) at 20× zoom and backlit using a transmitted light stage connected to a halogen light source (model KL 1500 LCD, Schott, Germany). Adobe Photoshop (version CS6) was used to blend images into one combined image for each cross-section (Fig. S4) [**Supplementary Information**], and the analysis of filled vessels was completed using ImageJ (Schneider et al., 2012) to count silicone-filled vessels in each image and quantify the area of silicone-filled vessels in each image both in mm^2 and as percent of the total xylem area. The silicone-filled vessel volume was calculated from these data by linear interpolation between each cross-section (Fig. S5) [**Supplementary Information**]. Counts of filled vessels (C) at each distance (d) from the injected surface were used to estimate median vessel lengths, based on fitting the equation $\ln C = a + b \times d$ using the software TableCurve 2D (version 5.01, Systat, San Jose, CA, USA).

Mass spectrometry

Direct-infusion electrospray ionization triple-quadrupole mass spectrometry was performed using an Applied Biosystems API 4000 as described by Shiva et al. (2013). The dried samples (n = 3 per species), each originating from 2 mL or 4 ml of xylem sap or cell contamination control (see breakdown of species above), were dissolved in 1 ml chloroform in a 2 mL glass vial, where the solvent was evaporated under nitrogen. 1.2 mL of chloroform:methanol:300 mM ammonium acetate in water (30:66.5:3.5) containing internal standards were added, and the mixture was vortexed. Internal standards and the amounts used are shown in Table S1 [**Supplementary Information**]. In addition to the scans described in Shiva et al. (2013), a scan for SQDG (Pre 225.0) in negative ion mode (Welti et al., 2003) was also acquired (except for samples from *Laurus* and *Bambusa*). Data were processed as described in Shiva et al. (2013) using the LipidomeDB Data Calculation Environment at http://129.237.137.125:8080/Lipidomics/ (Zhou et al., 2011).

Confocal laser scanning microscopy

To test for lipids in xylem of *Laurus*, fluorescent FM1-43 dye (Molecular Probes, Life Technologies, Eugene, OR, USA) was infiltrated into living xylem and imaged with laser scanning confocal microscopy, as described in Schenk et al. (2018). FM1-43 is an amphiphilic fluorophore that is virtually non-fluorescent in water and strongly fluorescent under cyan light excitation when bound to lipids, including amphiphilic lipids, and biological membranes (Jelínková et al., 2010). It was used as a 5 µg/mL solution in nanopure water with 488 nm excitation and an emission window of 578 to 618 nm. Woody stems, approximately 5-8 mm in diameter and about 10 cm long, were cut from the plants and submerged in DI water. About 2.5 cm were cut under water from each end of the stem to remove most bubbles in the xylem that may have been induced by the cutting. The cut ends were then recut with new razor blades to

create clean and smooth surfaces. Bark was removed from about 1 cm length at the distal end to expose the xylem. The proximal end of each stem was connected to a vacuum flask using tight-fitting latex tubing around the stem inside Tygon tubing. A short piece of Tygon tubing was fitted to the exposed xylem cylinder at the distal end, using latex tubing around the cylinder to create a tight fit. The distal cut end was cleaned by washing it three times with 500 µL nanopure water using a pipette. 1 mL of fluorophore solution was then added into the tubing and onto the exposed xylem surface. Lab vacuum was turned on and turned off once the solution was absorbed into the xylem, but no air was aspirated. The control was treated the same way but, instead of the fluorophore solution, 1 mL of nanopure water was sucked through the stem. A 2 mm long stem piece was then cut along its transverse plane from the center of the stem segment and the distal surface recut using a sledge microtome (Sledge microtome GSL 1, Schweingruber, Switzerland). The stem piece was then placed onto a cell culture dish with a glass bottom of 175 µm (CELLview™ dish, Greiner Bio-One, Germany) in a drop of water and observed using the inverted microscope of a confocal laser scanning microscope (model TCS SP8 with a HyVolution super-resolution detector, Leica Microsystems, Wetzlar, Germany). Lignin was detected with 405 nm excitation and an emission window of 467 to 509 nm. Imaging was done with a 63.0 × 1.20 objective and 3× digital zoom in water, using four scans per image at 1760 × 1760 resolution.

Transmission electron microscopy (TEM)

Small sectioning blocks of xylem from fresh *Laurus* stems were given two different treatments as described in Schenk et al. (2017): (1) fixation with a solution containing 2.5% glutaraldehyde, 1% sucrose, and 0.1 M phosphate buffer at pH 7.3, and (2) fixation with glutaraldehyde and then postfixation with a 2% aqueous osmium tetroxide (OsO_4) solution for 2 hours at room

temperature. The samples were dehydrated through a gradual ethanol series and embedded in Epon resin. Moreover, samples treated with glutaraldehyde only were observed with and without post staining of TEM grids with aqueous uranyl acetate and lead citrate to test the potential staining effect on vessel-vessel pit membranes (Ellis, 2014). The duration of the staining was 5 minutes for uranyl acetate and 1 minute for lead citrate. Transverse semi-thin sections were cut with an ultramicrotome (Leica Ultracut UCT, Leica Microsystems, Vienna, Austria), stained with 0.5% toluidine blue in 0.1 M phosphate buffer, and mounted on microscope slides using Eukitt. Ultra-thin sections between 60 nm and 90 nm were mounted on copper grids (Athena, Plano GmbH, Wetzlar, Germany) and observed with a JEM-1210 TEM (Jeol, Tokyo, Japan) at 120 kV. Digital images were taken using a MegaView III camera (Soft Imaging System, Münster, Germany).

RESULTS

Xylem sap lipidomics

Lipids extracted from xylem sap and cell contamination controls included the galactolipids digalactosyldiacylglycerol (DGDG) and monogalactosyldiacylglycerol (MGDG), as well as all common plant phospholipids. Total lipid concentrations for xylem sap varied between 0.18 µmol / L for *Laurus* and *Liriodendron* and 0.63 µmol / L for *Bambusa*, averaging 0.41 (± 0.17 SD) µmol / L across species (Fig. 1). Lipid concentrations in cell contamination controls ranged from 1.1% of the amount detected in xylem sap in *Distictis* to 9.0% in *Laurus*, averaging 4.49 (± 2.80 SD) percent across species. The most pronounced differences in chemical compositions between species were in the amounts of galactolipids as a percentage of total lipids (*Laurus* 75.4%, *Liriodendron* 35.9%, *Bambusa* 57.0%, *Triadica* 18.8%, *Geijera* 10.6%, *Distictis* 20.4%, *Encelia* 7.1%). Sulfolipids were detected only in trace amounts. The complete lipidomics data set may be

SUBMITTED MANUSCRIPT

found in Table S2 for xylem sap and Table S3 for cell contamination controls [**Supplementary Information**]. Lipid concentrations in sap were not statistically related to the vessel volume opened by cutting stems, but the two species with the lowest vessel lipid concentrations, *Liriodendron* and *Laurus*, also had among the lowest vessel volumes (Fig. 2). Lipid concentrations in the sap of the other five species were similar (Fig. 2), even though *Encelia* had a very low vessel volume and *Distictis* by far the highest vessel volume.

The most common lipids grouped by their head groups (Fig. 1) were DGDG, MGDG, phosphatidylcholine (PC), phosphatidic acid (PA), phosphatidylethanolamine (PE), phosphatidylinositol (PI), with other phospholipids present in much lower amounts, including phosphatidylserine (PS), phosphatidylglycerol (PG), lysophosphatidylethanolamine (LPE), lysophosphatidylcholine (LPC), and lysophosphatidylglycerol (LPG). Trace amounts of a contaminant that was also found in solvent controls, and therefore most likely originated from a solvent, interfered with the detection of LPG, which was therefore excluded from all figures and analyses.

Overall, the lipid compositions in xylem sap across species were fairly similar, with the most pronounced differences between species found in the percentages contributed by DGDG, MGDG, PC, and PA (Fig. 1). DGDG varied from about 3.0% of all lipids in *Encelia* to 32.0% in *Bambusa*, with a mean across species of 12.4 (± 10.5 SD)%; MGDG varied from 4.1% in *Encelia* to 54.6% in *Laurus*, with a mean across species of 19.8 (±17.8 SD)%; PC varied from 12.3% in *Laurus* to 30.1% in *Triadica*, with a mean across species of 18.2 (±6.3 SD)%; PA varied from 1.9% in *Laurus* to 50.6% in *Encelia*, with a mean across species of 28.7 (±17.6 SD)%.

The most common number of acyl chain carbon atoms were 34 and 36, with galactolipids mostly having more 36-carbon combinations than phospholipids (Fig. 3). Only on average 1.56 (± 0.70 SD)% of all lipids were fully saturated phospholipids, and the most common numbers of double bonds were 1-3 for 34 carbon atom acyl chains and 3-5 for 36 carbon atom acyl chains (Fig. 3).

SUBMITTED MANUSCRIPT

Averaged across species, lipids with 34:1-3 (carbon atoms:number of double bonds) and 36:3-5 accounted for 84.0 (± 4.9 SD)% of all apoplastic xylem lipids. The lipid composition of the galactolipids, with a total of 4 double bonds prominent, suggests that 18:2 and/or 18:1 fatty acids are common.

Visualization of lipids in xylem vessels

Treatment with FM1-43 showed continuous lipid layers on vessel surfaces of *Laurus nobilis*, with high concentrations in inter-vessel pits (Fig. 4A-B). Pit membranes were clearly visible under confocal laser scanning microscopy as thick, pillow-shaped, black structures with lipid coatings on either side and some faint labelling inside the membranes. Never-dried pit membranes of *Laurus* were 1,252 nm (± 238 nm, standard deviation; n = 36 pit membranes) thick under confocal microscopy (Fig. 4A-B), but 601 nm (± 150 nm; n = 19) under TEM (Fig. 4D-G), showing that the dehydration required for TEM by propanol could result in shrinkage of the pit membrane. These observations were very similar to those published previously for five of the other study species, including *Liriodendron*, *Triadica*, *Geijera*, *Distictis*, and *Encelia* (Schenk et al., 2018). As previously observed, the lipid layer appears broken up into aggregates under TEM (Fig. 4F-G) but was found in a continuous layer in the same locations observed under confocal microscopy on vessel and pit surfaces and on the pit membrane (Fig. 4A-B).

DISCUSSION

The most important take-home message of this study is that amphiphilic lipids exist in xylem conduits across the angiosperm phylogeny, including basal angiosperms (magnoliids), monocots, and eudicots. Phospholipids have been found in xylem sap before (Gonorazky et al., 2012, Schenk et al., 2017), but this is the first lipidomic analysis of xylem sap for multiple species and the first report of galactolipids anywhere in the plant apoplast. These findings raise questions about the functions of these lipids in xylem conduits of angiosperms.

Chemical composition of xylem sap lipids

The concentrations of lipids in xylem sap were surprisingly consistent across species, with the two species from the magnoliid clade, *Laurus* and *Liriodendron*, having about a third of the concentrations of the other five species (Fig. 1). Because lipid micelles or lipid-coated gas bubbles in xylem sap are mostly larger than 50 nm in diameter (Schenk et al., 2017) and therefore too large to pass through pit membrane pores, which do not exceed 20 nm in hydrated pit membranes (Choat et al., 2003, Zhang et al., 2017), it is likely that the observed xylem sap lipids originate largely from conduits cut open for the sap extraction. To account for this, we analysed the vessel volumes of the seven species and found no significant relationship between lipid concentrations in sap and vessel volumes (Fig. 2). However, it is worthy of note that the desert shrub *Encelia* had high lipid concentration despite having the smallest vessel volume and the tropical liana *Distictis* did not have the highest lipid concentrations, despite having much larger vessel volume than any of the other species (Fig. 2). These findings could have something to with the environmental conditions in which these species are found.

Lipids are insoluble and in xylem conduits most are attached to surfaces (Fig. 4; Schenk et al., 2018), so the amounts extracted in sap may only be a small fraction of all apoplastic xylem lipids. Quantification of all apoplastic lipids in xylem would require either complete extraction from individual conduits with organic solvents and/or detergents, which could cause artifacts if these substances penetrated into living vessel-associated cells (Morris et al., 2018b), or quantification of lipids in vessel images via mass spectrometry imaging (Ellis et al., 2013).

The very low concentrations of lipids found in cell contamination controls show that at least 95% of the lipids in xylem sap samples did not originate from cut parenchyma cells at the xylem surface. *Bambusa* and *Distictis*, both of which have phloem embedded with xylem (*Distictis* has intraxylary phloem) had the lowest percentages of lipid concentrations in their control samples (4.3% in *Bambusa* and 1.1% in *Distictis*), demonstrating that hardly any lipids in xylem sap samples originated from the phloem.

SUBMITTED MANUSCRIPT

The only other lipidomic analysis of xylem sap, for tomato (Gonorazky et al., 2012), did not include analyses of galactolipids, but the chemical composition of phospholipids was roughly comparable to our findings, with PC and PA being the most abundant phospholipids. The xylem sap concentration of phospholipids in tomato (0.037 µmol kg^{-1}) was similar to concentrations in *Laurus* (0.044 µmol L^{-1}), but much lower than the average phospholipid concentrations across all species studied (0.296 ± 0.161 SD µmol L^{-1}).

The presence of the galactolipids DGDG and MGDG in the xylem apoplast is especially notable, because galactolipids are synthesized exclusively in plastids (Dörmann and Benning, 2002, Botté and Maréchal, 2014) and are the most abundant lipids in chloroplasts, but they have never been found in any apoplastic compartment, presumably because there have been so few studies of "the black box of plant apoplast lipidomes" (Misra, 2016). Moreover, their physical properties, such as interactions of the head-groups with water molecules, are different from phospholipids (Kanduč et al., 2017). MGDG have very small head-groups and form bilayers only in mixture with other lipids (Dörmann and Benning, 2002), where interactions between MGDG and DGDG head groups affect the physical properties of galactolipids at gas-water interfaces (Bottier et al., 2007). Because galactolipids originate from plastids, it is also notable that sulfolipids, which are abundant in plastids (Shimojima, 2011), were only found in trace amounts in xylem sap.

Regarding acyl chain configurations, it was observed that galactolipids mostly had 36-carbon combinations, most likely consisting of two 18-carbon chains (Fig. 3). All seven species studied are from plant families that synthesize fatty acids for galactolipids mostly in the ER, resulting in 18:3 fatty acid chains in galactolipids (Mongrand et al., 1998). The lipid composition of the galactolipids, with a total of 4 double bonds prominent, suggests that 18:2 and/or 18:1 fatty acids are common. Whole tissue data demonstrate that generally shoots are very high in 18:3, while roots and seeds are less unsaturated with more 18:2 and 18:1-containing galactolipids (Devaiah et al., 2006, Huynh et al., 2012).

The chemical composition of lipids in xylem sap is different from that found in any cell compartment. Galactolipids made up 75.4% of all lipids in *Laurus* sap, which is similar to the percentage found in chloroplasts (Dörmann and Benning, 2002), but mostly the mixture of phospho- and galactolipids in sap was different from that found in any cellular or plastid membrane bilayer. The properties of such mixtures when forming monolayers, bilayers and micelles have never been studied before. Clearly there is an urgent need for research on the dynamic surface tension and molecular structure of different mixtures of phospho- and galactolipids at gas-water interfaces to explore their functions in xylem and possible roles in gas bubble formation. There may also be important roles for xylem proteins in the structure and dynamics of lipid layers in conduits, as found for pulmonary lipid layers (Pérez-Gil, 2008, Parra and Pérez-Gil, 2015). Proteins are abundant in xylem sap (Buhtz et al., 2004) and in pit membranes (Harrak et al., 1999, Neumann et al., 2010, Schenk et al., 2018) and are likely to interact with lipids there.

Besides finding galactolipids in xylem sap, the presence of phosphatidic acid (PA) at high concentrations in some species is also notable (Fig. 1). High concentrations of PA in plant samples are usually attributed to phospholipase D (PLD) activity, which cleaves the choline head-group off phosphatidylcholine (PC) and some head groups off other phospholipids to create PA (Christie, 1993, Welti et al., 2002). PLD is active when bound to cell membranes (Kolesnikov et al., 2012), and cutting living cells causes PLD activation as part of a wounding response (Bargmann et al., 2009). Therefore, high PA concentrations can be artifacts of wounding, and very thorough cleaning of cut xylem surfaces is therefore essential for keeping fragments of cell membranes containing PLD out of xylem sap collections. PLD can remain active even in organic solvents such as chloroform:methanol (Christie, 1993), possibly because membrane fragments form inverted vesicles in organic solvents that allow for continued PLD activity in the hydrophilic interior of the vesicle, as has been suggested for phospholipase C (PLC) (Kates, 1957).

The high PA concentrations found in xylem sap of some species, such as *Encelia*, *Geijera*, and *Distictis* (Fig. 1) were initially a concern, because it was suspected that they could be sampling artifacts. However, treatments of cut xylem surfaces with the PLD inhibitors 1-butanol, 5-fluoro-2-indolyl des-chlorohalopemide (FIPI) (Su et al., 2009), and a lipase inhibitor cocktail (Furse et al., 2013) had no effect on PA concentrations in xylem sap of *Distictis* (data not shown). Moreover, PLD or other phospholipases have never been detected in proteomic analyses of xylem sap (Alvarez et al., 2006, Djordjevic et al., 2007, Aki et al., 2008, Krishnan et al., 2011, Ligat et al., 2011, Dugé de Bernonville et al., 2014), which may not be surprising, because PLD is often bound to membranes and therefore unlikely to occur naturally in xylem sap.

These lines of argument all support PA as a natural ingredient of xylem sap in most of the species studied (Fig. 1). PA has also been found in relatively high concentrations in xylem sap of tomato plants (Gonorazky et al., 2012). PA has many functions in plants, interacts with many proteins, and has important roles in lipid metabolism and signalling (Testerink and Munnik, 2011), wounding responses (Bargmann et al., 2009), and in responses to stress, such as drought and salinity (McLoughlin and Testerink, 2013). The physical properties of PA are also unique when compared to other amphiphilic lipids in having the smallest and negatively charged head-group, binding of cations such as Ca^{2+} and Mg^{2+} (Ohki and Ohshima, 1985), and causing PA to have lower surface tension in monolayers than other phospholipids (Weschayanwiwat et al., 2005). Of all the various roles of PA, its interactions with cations and effects on surface tension in the presence of gas interfaces are likely to be most important in the xylem apoplast environment.

The amounts of choline-containing phospholipids (PC and LPC) found in xylem sap were much lower than estimated in previous research using an enzymatic assay (Schenk et al., 2017), where all choline quantified in xylem sap was assumed to originate via PLD activity from choline-containing phospholipids. However, even if all PA found in xylem sap in this study originated from choline-containing phospholipids, then PC, LPC, and PA together would still account for

SUBMITTED MANUSCRIPT

less than 20% of the choline concentrations found previously in xylem sap by Schenk et al. (2017). We therefore conclude that the concentration estimates for choline-containing phospholipids in our previous paper were much too high, and this is also supported by a re-examination of the data from Schenk et al. (2017) for choline concentrations in xylem sap that was not treated with PLD, which ranged from 0.44 µmol L^{-1} for *Distictis* to 1.56 µmol L^{-1} for *Geijera*, averaging 1.06 µmol L^{-1} across all five species studied, which is more than twice the molar concentration of all lipids in xylem sap combined. Xylem sap choline could potentially originate from PLC activity acting on lipids attached to xylem surfaces (Fig. 4; Schenk et al., 2016). More research is required to explore that possibility.

Where do apoplastic xylem lipids come from?

There are two possible and not mutually exclusive origins for apoplastic xylem lipids: The lipids may remain from the living cell content of conduits (Scott et al., 1960, Esau et al., 1966), including their plastids, which would explain the presence of galactolipids in xylem sap. Lipids could also be transported into conduits from conduit-associated parenchyma cells (Czaninski, 1977, Morris et al., 2018b). This would require transport of lipids across the protective layer surrounding such cells, which consists mainly of polysaccharides (Chafe and Chauret, 1974, Fujii et al., 1981, Wisniewski et al., 1991a, Wisniewski et al., 1991b, Wisniewski and Davis, 1995), as well as across the pit membrane, which mainly consists of cellulose. The transport could involve non-specific lipid transfer proteins (nsLTPs), which can transport lipids across cell walls (Domínguez et al., 2015, Fich et al., 2016, Li et al., 2016, Misra, 2016) and which have been found in xylem cell walls and xylem sap (Buhtz et al., 2004, Djordjevic et al., 2007, Krasikov et al., 2011, Ligat et al., 2011).

One major difference between these two origins of apoplastic lipids is that transport from conduit-associated cells would allow for changes in lipid concentration and composition in conduits seasonally or in response to environmental conditions, which could possibly affect hydraulic functions and embolism resistance. Plants species vary widely in the amount and

SUBMITTED MANUSCRIPT

degree of contact between conduits and living parenchyma cells in secondary xylem (Martínez-Cabrera et al., 2009, Morris et al., 2015, Morris and Jansen, 2016, Morris et al., 2018a), and it could be that some species transport lipids into conduits while others do not. Seasonal changes in the electron-density of pit membranes have been observed (Schmid and Machado, 1968), and this could potentially indicate lipid accumulation in conduits over time.

Apoplastic xylem lipids and functional implications

The presence of lipids on xylem conduit surfaces and pit membranes is incompatible with the widely accepted assumption that gas bubble formation in xylem is prevented by the high surface tension of water (Oertli, 1971, Sperry and Tyree, 1988, Tyree and Zimmermann, 2002, Stroock et al., 2014). There is unequivocal evidence for negative pressure in xylem, and the validity of the CT theory is not in question (Jansen and Schenk, 2015, Schenk et al., 2015, Schenk et al., 2017, Venturas et al., 2017). However, assumptions about bubble formation in xylem under negative pressure may have to be revisited, because layers of phospho- and galactolipids on conduit surfaces and in pit membranes are certain to reduce the surface tension at gas-water interfaces substantially below that of pure water, with the dynamic surface tension depending on the local concentration of lipids at the surface (Zuo et al., 2004, Kwan and Borden, 2010). Surface tension of xylem sap residue has been found to be strongly concentration-dependent and as low as $1/10^{th}$ that of water at high concentration (Schenk et al., 2017). So how do amphiphilic lipids that are concentrated in pits (Fig. 4; Schenk et al., 2018) affect bubble formation via air seeding from pit membrane pores?

In an earlier paper, we proposed a hypothesis to reconcile the presence of apoplastic xylem lipids with the CT theory (Schenk et al., 2015) and later amended and modified that hypothesis in the light of new data (Schenk et al., 2017). To summarize that hypothesis briefly, gas penetrating from embolized conduits into pit membranes of sap-filled conduits may snap off nanobubbles inside confined, lipid-coated pore spaces, resulting in the creation of lipid-coated nanobubbles (Fig. 5), which have in fact been found in xylem sap (Schenk et al., 2017). Key to this hypothesis

is that both the low dynamic surface tension of lipids and the formation inside pit membrane pores would limit the bubbles' sizes and keep them below a critical threshold that prevents bubble expansion into embolism (Schenk et al., 2015, Schenk et al., 2017). This process could happen under normal xylem water potentials and would allow xylem to operate without spreading embolisms via air seeding from gas-filled conduits. The population of lipid-coated nanobubbles could also function as a gas reservoir that serves as a buffer when dissolved gas in sap exceeds saturation under increasing temperatures (Schenk et al., 2016).

Below a more negative air seeding pressure threshold, gas could still penetrate through the entire length of pit membrane pores, causing a growing bubble to emerge from the pit membrane, where nothing would restrict the bubble's growth and resulting in embolism. This is the widely accepted air seeding mechanism (Sperry and Tyree, 1988, Tyree and Zimmermann, 2002, Stroock et al., 2014, Brodribb et al., 2016), which is supported by a large body of research. What the new lipid-nanobubble hypothesis could explain is how plants can operate under negative pressure at all without forming embolism even under mildly negative pressure, a feat that engineers have found almost impossible to replicate (Smith, 1994). If this hypothesis is correct, then lipids are required for water transport under negative pressure. More research on the functions of these lipids is clearly required.

Conclusions

This study provides conclusive evidence for substantial amounts of phospho- and galactolipids in xylem conduits across the whole angiosperm phylogeny, and these findings force major questions about the functions of these lipids for plant water transport and the cohesion tension theory, as well as about the origins of lipids. Research on the functions of lipids in water that is under negative pressure and in the presence of gas-water interfaces in pit membranes and bubbles will benefit from an interdisciplinary approach to involve surface scientists and physicists with expertise on the behavior of lipids at surfaces such as pulmonary surfactant layers (Zuo et al., 2008, Zhang et al., 2011, Kanduč et al., 2013, Kanduč et al., 2016). Moreover,

possible interactions between lipids and proteins in xylem conduits need to be investigated. Even in the absence of gas in conduits, lipids accumulated in pit membranes are likely to affect sap flow and could be involved in the regulation of hydraulic conductance, the so-called ionic effect (Nardini et al., 2011, Nardini et al., 2012). Finally, if lipids are crucial for plant water transport, then they should be found as well in gymnosperms, ferns, and perhaps even moss hydroids. The discovery, or rather rediscovery (Scott et al., 1960, Esau, 1965, Esau et al., 1966, Wagner et al., 2000), of lipids in xylem conduits opens a vast field of new research questions.

FUNDING

The research was funded by research grants from the National Science Foundation (EAGER IOS-1558108 and IOS- 1754850).

ACKNOWLEDGEMENTS

The authors thank Jessica Garcia, Ryan Cochoit, Kerri Mocko, Alec Hunt, and Tilly Duong for assistance with xylem sap extractions and vessel volume analyses, Jim Henrich at the Los Angeles County Arboretum and Greg Pongetti at the Fullerton Arboretum for allowing sampling of plants in their living collections, and the Electron Microscopy Section of Ulm University for preparing TEM samples.

LITERATURE CITED

Aki T, Shigyo M, Nakano R, Yoneyama T, Yanagisawa S. 2008. Nano scale proteomics revealed the presence of regulatory proteins including three FT-like proteins in phloem and xylem saps from rice. *Plant and Cell Physiology* **49**: 767-790.

Alvarez S, Goodger JQD, Marsh EL, Chen S, Asirvatham VS, Schachtman DP. 2006. Characterization of the maize xylem sap proteome. *Journal of Proteome Research* **5**: 963-972.

Angeles G, Bond B, Boyer JS, *et al.* 2004. The cohesion-tension theory. *New Phytologist* **163**: 451-452.

Askenasy E. 1895. Ueber das Saftsteigen. *Verhandlungen des Naturhistorisch-medizinischen Vereins zu Heidelberg, N.F.* **5**: 325-345.

Bargmann BOR, Laxalt AM, Riet BT, *et al.* 2009. Reassessing the role of phospholipase D in the *Arabidopsis* wounding response. *Plant, Cell & Environment* **32**: 837-850.

Botté CY, Maréchal E. 2014. Plastids with or without galactoglycerolipids. *Trends in Plant Science* **19**: 71-78.

Bottier C, Géan J, Artzner F, *et al.* 2007. Galactosyl headgroup interactions control the molecular packing of wheat lipids in Langmuir films and in hydrated liquid-crystalline mesophases. *Biochimica et Biophysica Acta (BBA) - Biomembranes* **1768**: 1526-1540.

Brodribb TJ, Bienaimé D, Marmottant P. 2016. Revealing catastrophic failure of leaf networks under stress. *Proceedings of the National Academy of Sciences* **113**: 4865-4869.

Buhtz A, Kolasa A, Arlt K, Walz C, Kehr J. 2004. Xylem sap protein composition is conserved among different plant species. *Planta* **219**: 610-618.

Chafe SC, Chauret G. 1974. Cell wall structure in the xylem parenchyma of trembling aspen. *Protoplasma* **80**: 129-147.

Choat B, Ball M, Luly J, Holtum J. 2003. Pit membrane porosity and water stress-induced cavitation in four co-existing dry rainforest tree species. *Plant Physiology* **131**: 41–48.

Christie WW. 1993. Preparation of lipid extracts from tissues. In: Christie WW, ed. *Advances in Lipid Methodology – Two*. Dundee: Oily Press.

Czaninski Y. 1977. Vessel-associated cells. *IAWA Bulletin* **1977**: 51-55.

Devaiah SP, Roth MR, Baughman E*, et al.* 2006. Quantitative profiling of polar glycerolipid species from organs of wild-type *Arabidopsis* and a PHOSPHOLIPASE Dα1 knockout mutant. *Phytochemistry* **67**: 1907-1924.

Dixon HH, Joly J. 1895. On the ascent of sap. *Philosophical Transactions of the Royal Society of London, Series B* **186**: 563-576.

Djordjevic MA, Oakes M, Li DX, Hwang CH, Hocart CH, Gresshoff PM. 2007. The *Glycine max* xylem sap and apoplast proteome. *Journal of Proteome Research* **6**: 3771-3779.

Domínguez E, Heredia-Guerrero JA, Heredia A. 2015. Plant cutin genesis: unanswered questions. *Trends in Plant Science* **20**: 551-558.

Dörmann P, Benning C. 2002. Galactolipids rule in seed plants. *Trends in Plant Science* **7**: 112-118.

Dugé de Bernonville T, Albenne C, Arlat M, Hoffmann L, Lauber E, Jamet E. 2014. Xylem sap proteomics. In: Jorrin-Novo JV, Komatsu S, Weckwerth W, Wienkoop S, eds. *Plant Proteomics*: Humana Press.

Ellis EA. 2014. Staining sectioned biological specimens for transmission electron microscopy: conventional and en bloc stains. In: Kuo J, ed. *Electron Microscopy: Methods and Protocols.* 3rd ed. New York: Humana Press.

Ellis SR, Brown SH, in het Panhuis M, Blanksby SJ, Mitchell TW. 2013. Surface analysis of lipids by mass spectrometry: More than just imaging. *Progress in Lipid Research* **52**: 329-353.

Esau K. 1965. *Plant anatomy.* New York: John Wiley & Sons.

Esau K, Cheadle VI, Gill RH. 1966. Cytology of differentiating tracheary elements. II. Structures associated with cell surfaces. *American Journal of Botany* **53**: 765-771.

Espino S, Schenk HJ. 2011. Mind the bubbles: Achieving stable measurements of maximum hydraulic conductivity through woody plant samples. *Journal of Experimental Botany* **62**: 1119-1132.

Fich EA, Segerson NA, Rose JKC. 2016. The plant polyester cutin: Biosynthesis, structure, and biological roles. *Annual Review of Plant Biology* **67**: 207-233.

Fineran BA. 1997. Cyto- and histochemical demonstration of lignins in plant cell walls: an evaluation of the chlorine water ethanolamine silver nitrate method of Coppick and Fowler. *Protoplasma* **198**: 186-201.

Fujii T, Harada H, Saiki H. 1981. Ultrastructure of "amorphous layer" in xylem parenchyma cell wall of angiosperm species. *Mokuzai Gakkaishi* **27**: 149-156.

Furse S, Liddell S, Ortori CA*, et al.* 2013. The lipidome and proteome of oil bodies from *Helianthus annuus* (common sunflower). *Journal of Chemical Biology* **6**: 63-76.

Gascó A, Nardini A, Gortan E, Salleo S. 2006. Ion-mediated increase in the hydraulic conductivity of Laurel stems: role of pits and consequences for the impact of cavitation on water transport. *Plant Cell and Environment* **29**: 1946-1955.

Gonorazky G, Laxalt AM, Dekker HL*, et al.* 2012. Phosphatidylinositol 4-phosphate is associated to extracellular lipoproteic fractions and is detected in tomato apoplastic fluids. *Plant Biology* **14**: 41-49.

Greenidge KNH. 1952. An approach to the study of vessel length in hardwood species. *American Journal of Botany* **39**: 570-574.

Hacke UG, Sperry JS. 2003. Limits to xylem refilling under negative pressure in *Laurus nobilis* and *Acer negundo*. *Plant Cell and Environment* **26**: 303-311.

Harrak H, Chamberland H, Plante M, Bellemare C, Lafontaine JG, Tabaeizadeh Z. 1999. A proline-, threonine-, and glycine-rich protein down-regulated by drought is localized in the cell wall of xylem elements. *Plant Physiology* **121**: 557-564.

Huynh V-B, Repellin A, Zuily-Fodil Y, Pham-Thi A-T. 2012. Aluminum stress response in rice: effects on membrane lipid composition and expression of lipid biosynthesis genes. *Physiologia Plantarum* **146**: 272-284.

Jansen S, Schenk HJ. 2015. On the ascent of sap in the presence of bubbles. *American Journal of Botany* **102**: 1561-1563.

Jelínková A, Malínská K, Simon S*, et al.* 2010. Probing plant membranes with FM dyes: tracking, dragging or blocking? *The Plant Journal* **61**: 883-892.

Kanduč M, Schlaich A, de Vries AH*, et al.* 2017. Tight cohesion between glycolipid membranes results from balanced water–headgroup interactions. *Nature Communications* **8**: 14899.

Kanduč M, Schlaich A, Schneck E, Netz RR. 2016. Water-mediated interactions between hydrophilic and hydrophobic surfaces. *Langmuir* **32**: 8767-8782.

Kanduč M, Schneck E, Netz RR. 2013. Hydration interaction between phospholipid membranes: Insight into different measurement ensembles from atomistic molecular dynamics simulations. *Langmuir* **29**: 9126-9137.

Kates M. 1957. Effects of solvents and surface-active agents on plastid phosphatidase C activity. *Canadian Journal of Biochemistry and Physiology* **35**: 127-142.

Kolesnikov YS, Nokhrina KP, Kretynin SV*, et al.* 2012. Molecular structure of phospholipase D and regulatory mechanisms of its activity in plant and animal cells. *Biochemistry (Moscow)* **77**: 1-14.

Krasikov V, Dekker HL, Rep M, Takken FLW. 2011. The tomato xylem sap protein XSP10 is required for full susceptibility to *Fusarium* wilt disease. *Journal of Experimental Botany* **62**: 963-973.

Krishnan HB, Natarajan SS, Bennett JO, Sicher RC. 2011. Protein and metabolite composition of xylem sap from field-grown soybeans (*Glycine max*). *Planta* **233**: 921-931.

Kwan JJ, Borden MA. 2010. Microbubble dissolution in a multigas environment. *Langmuir* **26**: 6542-6548.

Li N, Xu C, Li-Beisson Y, Philippar K. 2016. Fatty acid and lipid transport in plant cells. *Trends in Plant Science* **21**: 145-158.

Ligat L, Lauber E, Albenne C*, et al.* 2011. Analysis of the xylem sap proteome of *Brassica oleracea* reveals a high content in secreted proteins. *Proteomics* **11**: 1798-1813.

Martínez-Cabrera HI, Jones CS, Espino S, Schenk HJ. 2009. Wood anatomy and wood density in shrubs: Responses to varying aridity along transcontinental transects. *American Journal of Botany* **96**: 1388-1398.

McLoughlin F, Testerink C. 2013. Phosphatidic acid, a versatile water-stress signal in roots. *Frontiers in Plant Science* **4**: 525.

Misra BB. 2016. The black-box of plant apoplast lipidomes. *Frontiers in Plant Science* **7**: 323.

Mongrand S, Bessoule J-J, Cabantous F, Cassagne C. 1998. The C16:3\C18:3 fatty acid balance in photosynthetic tissues from 468 plant species. *Phytochemistry* **49**: 1049-1064.

Morris H, Gillingham MAF, Plavcová L*, et al.* 2018a. Vessel diameter is related to amount and spatial arrangement of axial parenchyma in woody angiosperms. *Plant, Cell & Environment* **41**: 245-260.

Morris H, Jansen S. 2016. Secondary xylem parenchyma - from classical terminology to functional traits. *IAWA Journal* **37**: 1-15.

Morris H, Plavcová L, Cvecko P*, et al.* 2015. A global analysis of parenchyma tissue fractions in secondary xylem of seed plants. *New Phytologist* **209**: 1553-1565.

Morris H, Plavcová L, Gorai M*, et al.* 2018b. Vessel-associated cells in angiosperm xylem: Highly specialized living cells at the symplast-apoplast boundary. *American Journal of Botany* **105**: 153-162.

Nardini A, Dimasi F, Klepsch M, Jansen S. 2012. Ion-mediated enhancement of xylem hydraulic conductivity in four *Acer* species: relationships with ecological and anatomical features. *Tree Physiology* **32**: 1434-1441.

Nardini A, Salleo S, Jansen S. 2011. More than just a vulnerable pipeline: xylem physiology in the light of ion-mediated regulation of plant water transport. *Journal of Experimental Botany* **62**: 4701-4718.

Nardini A, Savi T, Losso A, *et al.* 2017. X-ray microtomography observations of xylem embolism in stems of *Laurus nobilis* are consistent with hydraulic measurements of percentage loss of conductance. *New Phytologist* **213**: 1068-1075.

Neumann PM, Weissman R, Stefano G, Mancuso S. 2010. Accumulation of xylem transported protein at pit membranes and associated reductions in hydraulic conductance. *Journal of Experimental Botany* **61**: 1711-1717.

Oertli JJ. 1971. The stability of water under tension in the xylem. *Zeitschrift für Pflanzenphysiologie* **65**: 195-209.

Ohki S, Ohshima H. 1985. Divalent cation-induced phosphatidic acid membrane fusion. Effect of ion binding and membrane surface tension. *Biochimica et Biophysica Acta* **812**: 147-54.

Parra E, Pérez-Gil J. 2015. Composition, structure and mechanical properties define performance of pulmonary surfactant membranes and films. *Chemistry and Physics of Lipids* **185**: 153-175.

Pérez-Gil J. 2008. Structure of pulmonary surfactant membranes and films: The role of proteins and lipid–protein interactions. *Biochimica et Biophysica Acta (BBA) - Biomembranes* **1778**: 1676-1695.

Schenk HJ, Espino S, Rich-Cavazos SM, Jansen S. 2018. From the sap's perspective: the nature of vessel surfaces in angiosperm xylem. *American Journal of Botany* **105**: 174-187.

Schenk HJ, Espino S, Romo DM, *et al.* 2017. Xylem surfactants introduce a new element to the cohesion-tension theory. *Plant Physiology* **173**: 1177-1196.

Schenk HJ, Espino S, Visser A, Esser BK. 2016. Dissolved atmospheric gas in xylem sap measured with membrane inlet mass spectrometry. *Plant, Cell & Environment* **39**: 944-950.

Schenk HJ, Steppe K, Jansen S. 2015. Nanobubbles: a new paradigm for air-seeding in xylem. *Trends in Plant Science* **20**: 199-205.

Schmid R, Machado RD. 1968. Pit membranes in hardwoods—Fine structure and development. *Protoplasma* **66**: 185-204.

Schneider CA, Rasband WS, Eliceiri KW. 2012. NIH Image to ImageJ: 25 years of image analysis. *Nature Methods* **9**: 671.

Schneider H, Manz B, Westhoff M*, et al.* 2003. The impact of lipid distribution, composition and mobility on xylem water refilling of the resurrection plant Myrothamnus flabellifolia. *New Phytologist* **159**: 487-505.

Scott FM, Sjaholm V, Bowler E. 1960. Light and electron microscope studies of the primary xylem of *Ricinus communis*. *American Journal of Botany* **47**: 162-173.

Shimojima M. 2011. Biosynthesis and functions of the plant sulfolipid. *Progress in Lipid Research* **50**: 234-239.

Shiva S, Vu HS, Roth MR*, et al.* 2013. Lipidomic analysis of plant membrane lipids by direct infusion tandem mass spectrometry. *Methods in Molecular Biology* **1009**: 79-91.

Smith AM. 1994. Xylem transport and the negative pressures sustainable by water. *Annals of Botany* **74**: 647-651.

Sperry JS, Hacke UG, Wheeler JK. 2005. Comparative analysis of end wall resistivity in xylem conduits. *Plant, Cell and Environment* **28**: 456-465.

Sperry JS, Tyree MT. 1988. Mechanism of water stress-induced xylem embolism. *Plant Physiology* **88**: 581-587.

Stroock AD, Pagay VV, Zwieniecki MA, Holbrook NM. 2014. The physicochemical hydrodynamics of vascular plants. In: Davis SH, Moin P, eds. *Annual Review of Fluid Mechanics, Vol 46*.

Su W, Yeku O, Olepu S, *et al.* 2009. 5-Fluoro-2-indolyl des-chlorohalopemide (FIPI), a Phospholipase D pharmacological inhibitor that alters cell spreading and inhibits chemotaxis. *Molecular Pharmacology* **75**: 437-446.

Testerink C, Munnik T. 2011. Molecular, cellular, and physiological responses to phosphatidic acid formation in plants. *Journal of Experimental Botany* **62**: 2349-2361.

Tyree MT, Salleo S, Nardini A, Lo Gullo MA, Mosca R. 1999. Refilling of embolized vessels in young stems of laurel. Do we need a new paradigm? *Plant Physiology* **120**: 11-21.

Tyree MT, Zimmermann MH. 2002. *Xylem structure and the ascent of sap.* Berlin: Springer-Verlag.

Venturas MD, Sperry JS, Hacke UG. 2017. Plant xylem hydraulics: What we understand, current research, and future challenges. *Journal of Integrative Plant Biology* **59**: 356-389.

Wagner HJ, Schneider H, Mimietz S, *et al.* 2000. Xylem conduits of a resurrection plant contain a unique lipid lining and refill following a distinct pattern after desiccation. *New Phytologist* **148**: 239-255.

Welti R, Li W, Li M, *et al.* 2002. Profiling membrane lipids in plant stress responses: Role of phospholipase Da in freezing-induced lipid changes in *Arabidopsis*. *Journal of Biological Chemistry* **277**: 31994-32002.

Welti R, Wang X, Williams TD. 2003. Electrospray ionization tandem mass spectrometry scan modes for plant chloroplast lipids. *Analytical biochemistry* **314**: 149-152.

Weschayanwiwat P, Scamehorn J, Reilly P. 2005. Surfactant properties of low molecular weight phospholipids. *Journal of Surfactants and Detergents* **8**: 65-72.

Westhoff M, Schneider H, Zimmermann D, *et al.* 2008. The mechanisms of refilling of xylem conduits and bleeding of tall birch during spring. *Plant Biology* **10**: 604-623.

Wheeler JK, Sperry JS, Hacke UG, Huang N. 2005. Inter-vessel pitting and cavitation in woody Rosaceae and other vesseled plants: a basis for a safety vs. efficiency trade-off in xylem transport. *Plant, Cell and Environment* **28**: 800-812.

Wheeler TD, Stroock AD. 2008. The transpiration of water at negative pressures in a synthetic tree. *Nature* **455**: 208-212.

Wisniewski M, Davis G. 1995. Immunogold localization of pectins and glycoproteins in tissues of peach with reference to deep supercooling. *Trees - Structure and Function* **9**: 253-260.

Wisniewski M, Davis G, Arora R. 1991a. Effect of macerase, oxalic acid, and EGTA on deep supercooling and pit membrane structure of xylem parenchyma of peach. *Plant Physiology* **96**: 1354-1359.

Wisniewski M, Davis G, Schaffer K. 1991b. Mediation of deep supercooling of peach and dogwood by enzymatic modifications in cell-wall structure. *Planta* **184**: 254-260.

Zhang H, Fan Q, Wang YE, Neal CR, Zuo YY. 2011. Comparative study of clinical pulmonary surfactants using atomic force microscopy. *Biochimica et Biophysica Acta (BBA) - Biomembranes* **1808**: 1832-1842.

Zhang Y, Klepsch M, Jansen S. 2017. Bordered pits in xylem of vesselless angiosperms and their possible misinterpretation as perforation plates. *Plant, Cell & Environment* **40**: 2133-2146.

Zhou Z, Marepally SR, Nune DS*, et al.* 2011. LipidomeDB data calculation environment: online processing of direct-infusion mass spectral data for lipid profiles. *Lipids* **46**: 879-84.

Zimmermann U, Schneider H, Wegner LH, Haase A. 2004. Water ascent in tall trees: does evolution of land plants rely on a highly metastable state? *New Phytologist* **162**: 575-615.

Zuo YY, Ding M, Li D, Neumann AW. 2004. Further development of Axisymmetric Drop Shape Analysis-Captive Bubble for pulmonary surfactant related studies. *Biochimica et Biophysica Acta (BBA) - General Subjects* **1675**: 12-20.

Zuo YY, Keating E, Zhao L*, et al.* 2008. Atomic force microscopy studies of functional and dysfunctional pulmonary surfactant films. I. Micro- and nanostructures of functional pulmonary surfactant films and the effect of SP-A. *Biophysical Journal* **94**: 3549-3564.

Zwieniecki MA, Melcher PJ, Holbrook NM. 2001. Hydrogel control of xylem hydraulic resistance in plants. *Science* **291**: 1059-1062.

FIGURE LEGENDS

FIG. 1. Chemical composition of xylem sap lipids as determined by direct-infusion electrospray ionization triple-quadrupole mass spectrometry. See Table S1 for the standards used and Tables S2 and S3 [**Supplementary Information**] for the complete data sets, including chains lengths and degrees of saturation. Sulfolipids were only found in trace amounts (Tables S2 and S3) and are not included in this figure.

FIG. 2. Most common numbers of acyl chain carbon atoms in xylem sap lipids and their degree of saturation (number of atoms:number of double bonds) as determined by direct-infusion electrospray ionization triple-quadrupole mass spectrometry. See Table S2 [**Supplementary Information**] for the complete data set.

FIG. 3. Total concentration of phospho- and galactolipids in xylem sap as a function of xylem vessel volume, shown here as vessel volume opened when cutting a stem relative to the xylem surface area. Numbers under the abbreviated genus names are the median vessel lengths in cm. Abbreviations: Bam = *Bambusa*, Dis = *Distictis*, Enc = *Encelia*, Gei = *Geijera*, Lau = *Laurus*, Lir = *Liriodendron*, Tri = *Triadica*.

FIG. 4. Lipids in xylem and inter-vessel pits of *Laurus nobilis*. A-C: Super-resolution confocal laser scanning microscopy images (false color) showing lignified cell walls in blue based on lignin autofluorescence and FM1-43 dye bound to lipids in yellow. White arrows = intervessel pit membranes. A-B: With FM1-43, C: Control without FM1-43. D-G: Transmission electron micrographs of intervessel pits. D-E: without OsO_4; showing unusually dark, electron-dense homogeneous pit membranes and linings on secondary walls, but no granular appearance. F-G: with OsO_4, lipids visible as black aggregates lining the wall surface, pit chamber and inside the pit membrane. Abbreviations: PA = pit aperture, PM = pit membrane, SW = secondary wall.

FIG. 5. Conceptual model of the formation of lipid-coated nanobubbles via snap-off inside pit membranes that are coated and infiltrated with surface-active lipids. The different sizes of micelles shown in this image reflect the wide range of nanoparticle sizes detected in xylem sap and presumed to be micelles and lipid-coated nanobubbles (Schenk et al. 2017).

SUBMITTED MANUSCRIPT

SUPPLEMENTARY MATERIALS

Table S1. Standards used for mass spectrometry of xylem sap lipids.

Table S2. Lipids in xylem sap (mean of n = 4, μmol L^{-1}).

Table S3. Lipids in cell contamination controls for xylem sap (mean of n = 4, μmol L-1).

Figure S4. Images of stems infiltrated with silicone.

Figure S5. Total vessel area filled with silicone as a function of distance from the infiltrated surface, shown for a sample of *Triadica sebifera*. The silicone-filled vessel volume was calculated from these filled areas by linear interpolation.

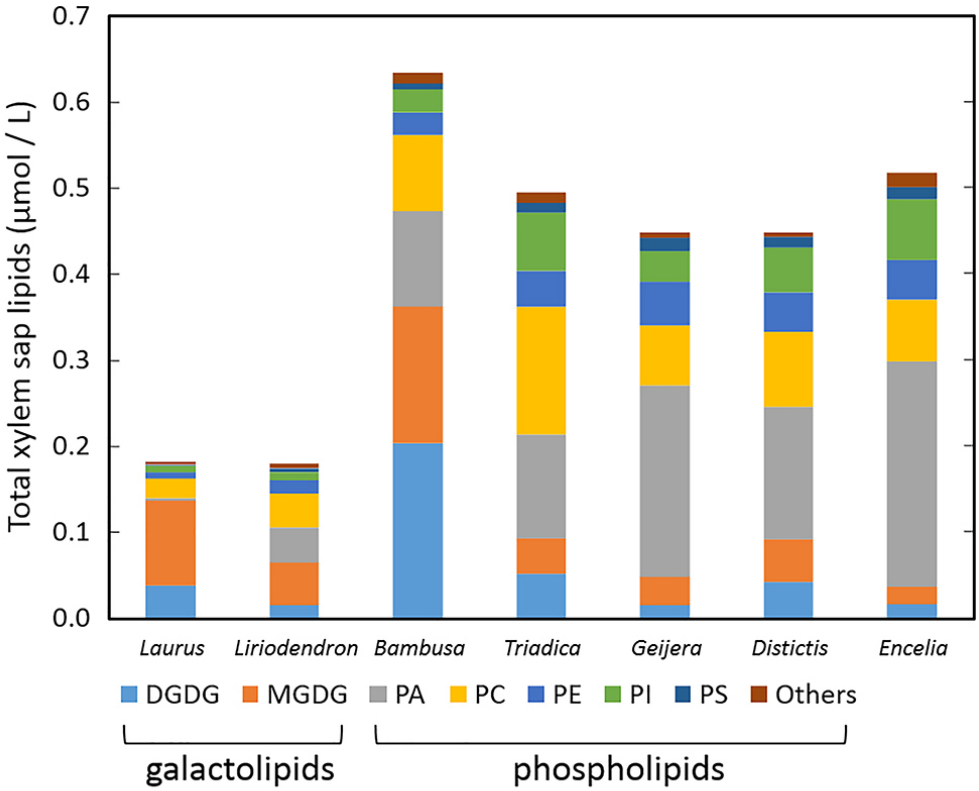

Fig. 1.

FIG. 1. Chemical composition of xylem sap lipids as determined by direct-infusion electrospray ionization triple-quadrupole mass spectrometry. See Table S1 for the standards used and Tables S2 and S3 [Supplementary Information] for the complete data sets, including chains lengths and degrees of saturation. Sulfolipids were only found in trace amounts (Tables S2 and S3) and are not included in this figure.

83x71mm (300 x 300 DPI)

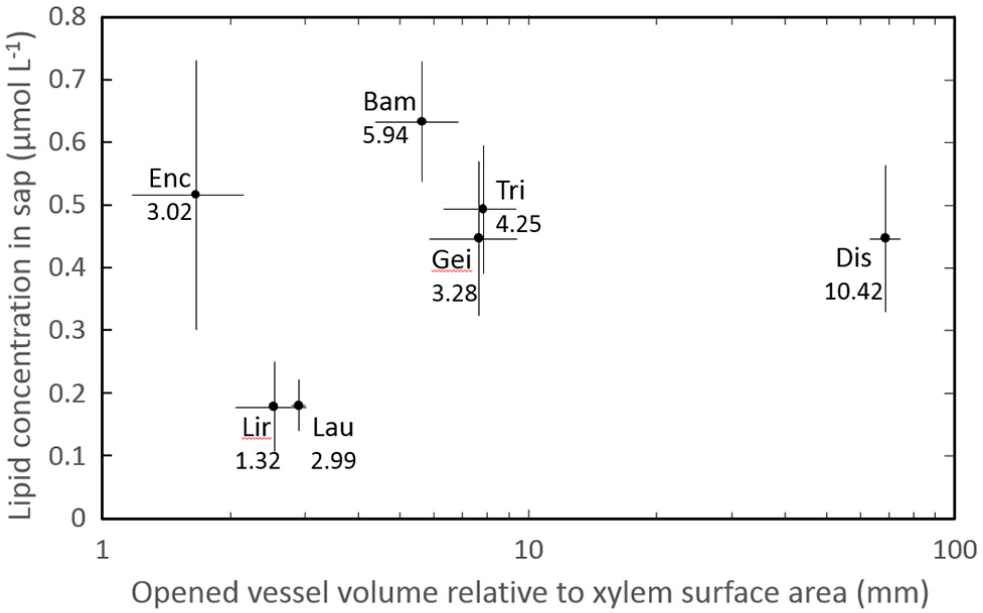

Fig. 2.

FIG. 2. Most common numbers of acyl chain carbon atoms in xylem sap lipids and their degree of saturation (number of atoms:number of double bonds) as determined by direct-infusion electrospray ionization triple-quadrupole mass spectrometry. See Table S2 [Supplementary Information] for the complete data set.

83x56mm (300 x 300 DPI)

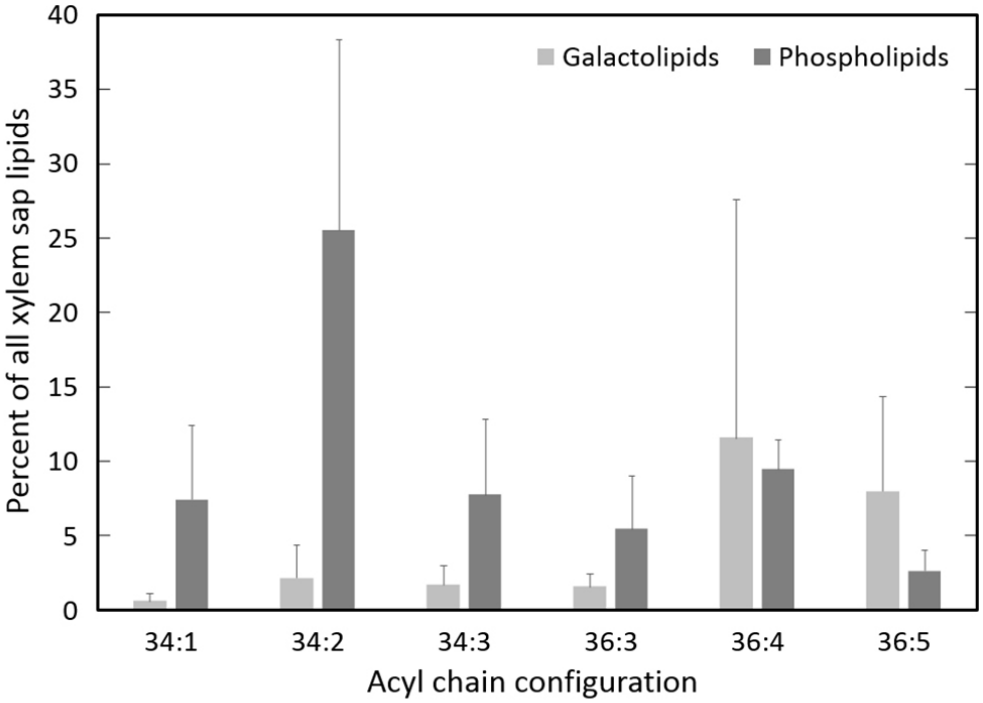

Fig. 3.

FIG. 3. Total concentration of phospho- and galactolipids in xylem sap as a function of xylem vessel volume, shown here as vessel volume opened when cutting a stem relative to the xylem surface area. Numbers under the abbreviated genus names are the median vessel lengths in cm. Abbreviations: Bam = Bambusa, Dis = Distictis, Enc = Encelia, Gei = Geijera, Lau = Laurus, Lir = Liriodendron, Tri = Triadica.

83x63mm (300 x 300 DPI)

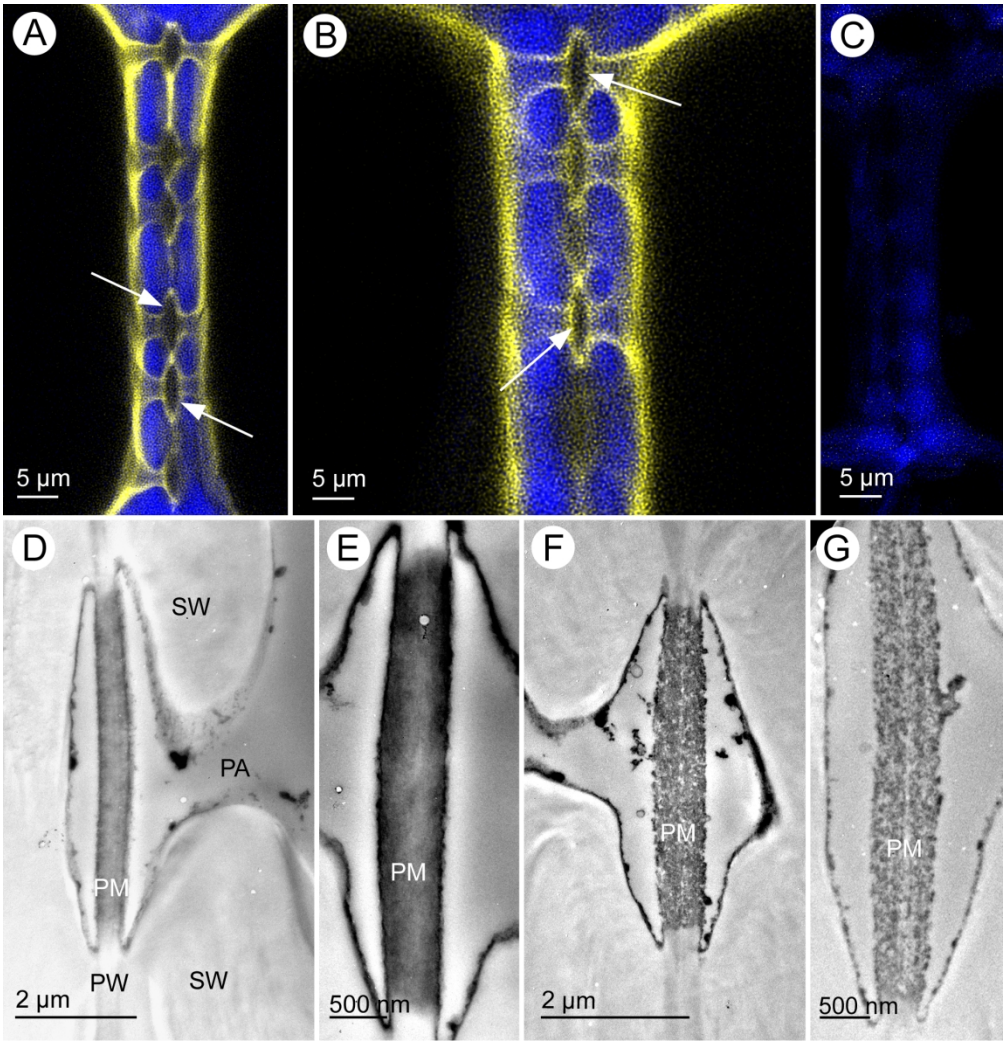

FIG. 4. Lipids in xylem and inter-vessel pits of Laurus nobilis. A-C: Super-resolution confocal laser scanning microscopy images (false color) showing lignified cell walls in blue based on lignin autofluorescence and FM1-43 dye bound to lipids in yellow. White arrows = intervessel pit membranes. A-B: With FM1-43, C: Control without FM1-43. D-G: Transmission electron micrographs of intervessel pits. D-E: without OsO4; showing unusually dark, electron-dense homogeneous pit membranes and linings on secondary walls, but no granular appearance. F-G: with OsO4, lipids visible as black aggregates lining the wall surface, pit chamber and inside the pit membrane. Abbreviations: PA = pit aperture, PM = pit membrane, SW = secondary wall.

172x178mm (300 x 300 DPI)

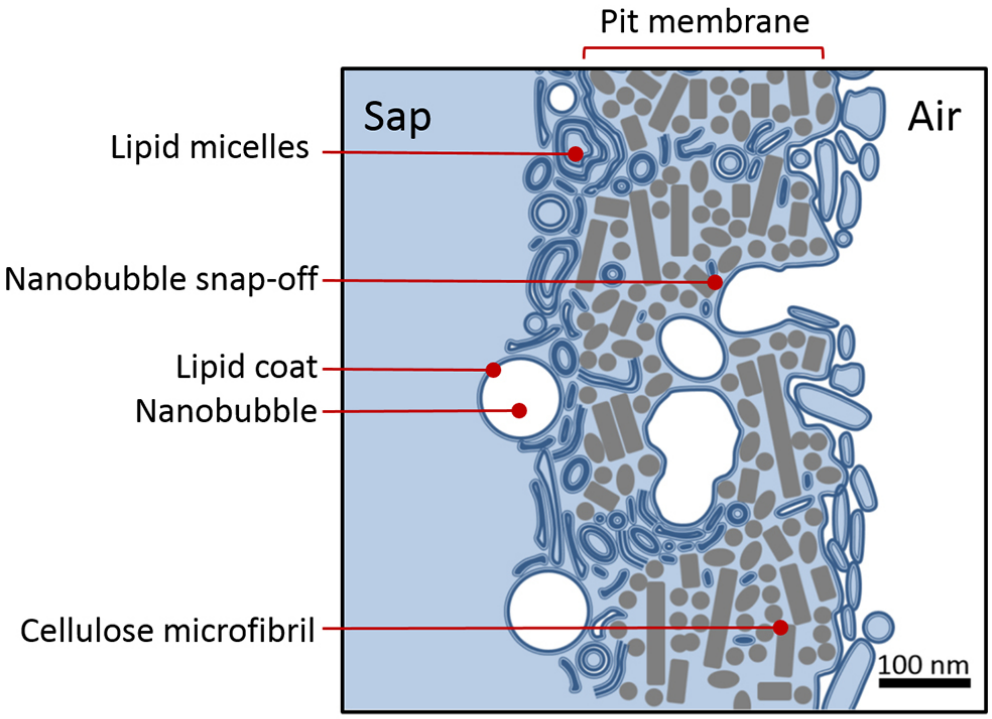

Fig. 5.

FIG. 5. Conceptual model of the formation of lipid-coated nanobubbles via snap-off inside pit membranes that are coated and infiltrated with surface-active lipids. The different sizes of micelles shown in this image reflect the wide range of nanoparticle sizes detected in xylem sap and presumed to be micelles and lipid-coated nanobubbles (Schenk et al. 2017).

83x66mm (300 x 300 DPI)

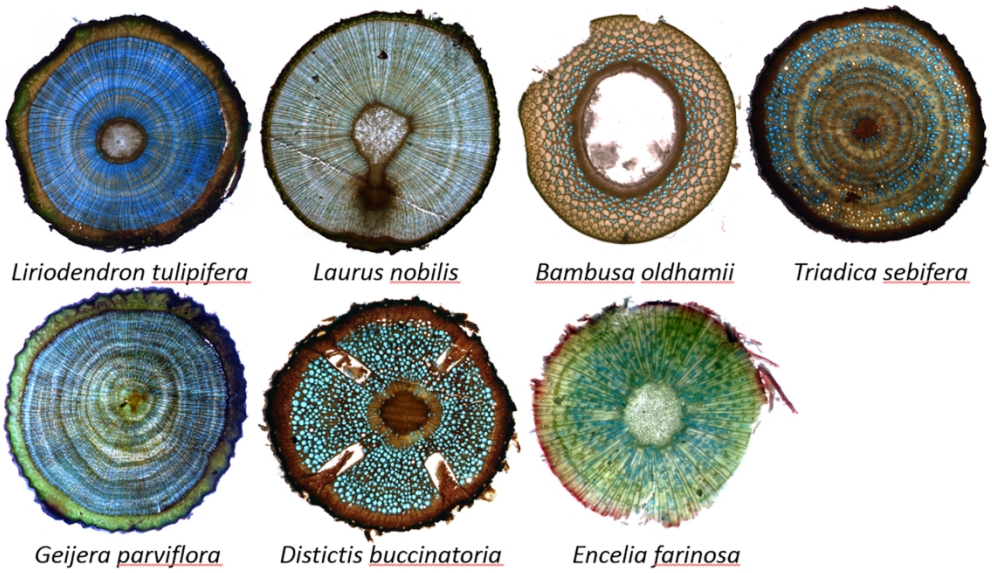

Fig. S4. Stems infiltrated with blue-colored silicone, cut at 0.7 cm from the injected surface. The four spoke-like structures in *Distictis buccinatoria xylem* are areas of interxylary phloem.

Figure S4. Images of stems infiltrated with silicone.

172x115mm (300 x 300 DPI)

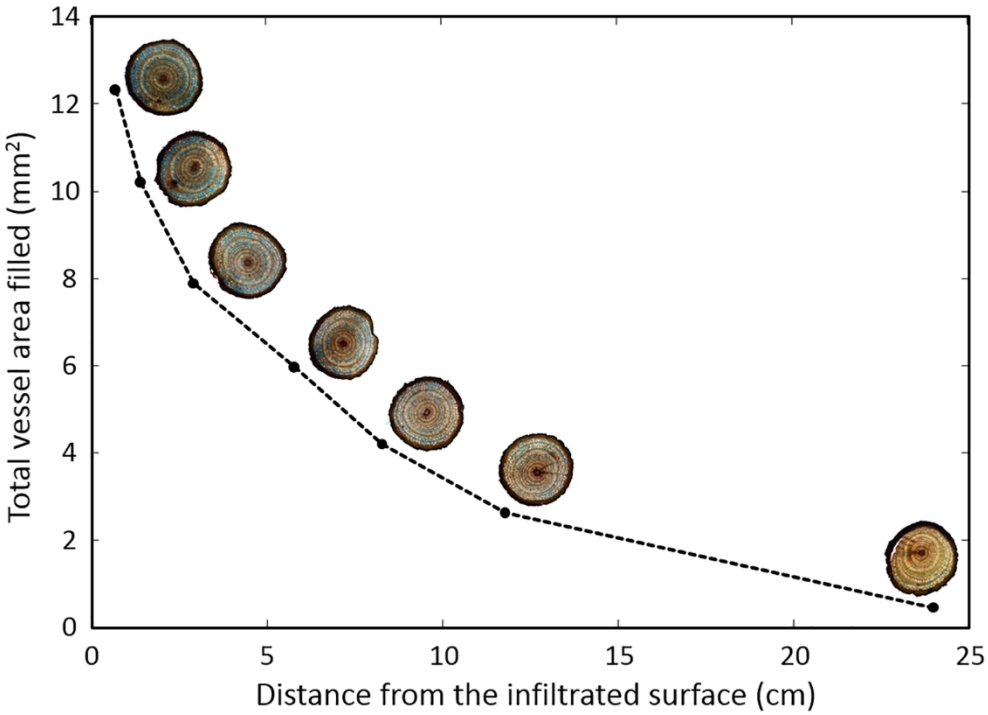

Fig. S5. Total vessel area filled with blue-colored silicone as a function of distance from the infiltrated surface, shown here for a sample of *Triadica sebifera*. The silicone-filled vessel volume was calculated from these filled areas by linear interpolation.

Figure S5. Total vessel area filled with silicone as a function of distance from the infiltrated surface, shown for a sample of Triadica sebifera. The silicone-filled vessel volume was calculated from these filled areas by linear interpolation.

172x138mm (300 x 300 DPI)

Table S1. Standards used for mass spectrometry of xylem sap lipids.

Internal standard	**Amount added (nmol)**	**Standard for**
	Phospholipids	
LPC (13:0)	0.300	LPC
LPC (19:0)	0.300	LPC
LPE (14:0)	0.150	LPE
LPE (18:0)	0.150	LPE
LPG (14:0)	0.150	LPG
LPG (18:0)	0.150	LPG
PA (14:0/14:0)	0.150	PA
PA (diphytanoyl, i.e., 20:0/20:0)	0.150	PA
PC (12:0/12:0)	0.300	PC
PC (24:1/24:1)	0.300	PC
PE (12:0/12:0)	0.150	PE
PE (diphytanoyl, i.e., 20:0/20:0)	0.150	PE
PG (14:0/14:0)	0.150	PG
PG (diphytanoyl, i.e., 20:0/20:0)	0.150	PG
PI (16:0/18:0)	0.144	PI
PI (18:0/18:0)	0.053	PI
PS (diphytanoyl, i.e., 20:0/20:0)	0.100	PS
PS14:0/14:0)	0.100	PS
	Galactolipids	
DGDG (18:0/16:0)	0.220	DGDG
DGDG (18:0/18:0)	0.740	DGDG
MGDG (18:0/16:0)	0.833	MGDG and SQDG
MGDG (18:0/18:0)	0.703	MGDG

SUBMITTED MANUSCRIPT

Table S2. Lipids in xylem sap (mean of n = 4, µmol L^{-1}). In parentheses: Number of carbon atoms in acyl chain:number of double bonds.

	Laurus nobilis		*Liriodendron tulipifera*		*Bambusa oldhamii*		*Triadica sebifera*		*Geijera parviflora*		*Distictis buccinatoria*		*Encelia farinosa*	
Compound*	**mean**	**std**	**mean**	**std**	**mean**	**std**	**mean**	**std**	**mean**	**std**	**mean**	**std**	**mean**	**std**
DGDG(34:4)	0.000	0.000	0.000	0.000	0.001	0.000	0.000	0.000	0.000	0.000	0.000	0.000	0.000	0.000
DGDG(34:3)	0.002	0.000	0.002	0.001	0.026	0.006	0.006	0.001	0.003	0.001	0.002	0.001	0.004	0.002
DGDG(34:2)	0.007	0.002	0.002	0.001	0.034	0.009	0.004	0.000	0.002	0.001	0.002	0.001	0.003	0.002
DGDG(34:1)	0.000	0.000	0.000	0.000	0.010	0.003	0.004	0.001	0.001	0.000	0.003	0.001	0.001	0.001
DGDG(36:6)	0.001	0.001	0.001	0.001	0.013	0.001	0.007	0.002	0.002	0.002	0.001	0.000	0.002	0.001
DGDG(36:5)	0.005	0.001	0.002	0.001	0.046	0.012	0.007	0.001	0.002	0.001	0.006	0.002	0.002	0.001
DGDG(36:4)	0.020	0.007	0.004	0.002	0.055	0.014	0.010	0.002	0.003	0.001	0.010	0.003	0.001	0.001
DGDG(36:3)	0.002	0.001	0.002	0.001	0.014	0.002	0.007	0.000	0.001	0.001	0.009	0.002	0.001	0.001
DGDG(36:2)	0.001	0.000	0.000	0.000	0.004	0.001	0.004	0.002	0.001	0.001	0.005	0.001	0.001	0.001
DGDG(36:1)	0.000	0.000	0.000	0.000	0.001	0.000	0.001	0.000	0.000	0.000	0.001	0.001	0.000	0.000
DGDG(38:6)	0.000	0.001	0.000	0.000	0.000	0.000	0.000	0.000	0.000	0.000	0.000	0.000	0.000	0.000
DGDG(38:5)	0.000	0.000	0.001	0.001	0.001	0.000	0.000	0.000	0.000	0.000	0.000	0.000	0.000	0.000
DGDG(38:4)	0.000	0.000	0.002	0.002	0.001	0.001	0.001	0.001	0.000	0.000	0.000	0.000	0.000	0.000
Total DGDG	**0.038**	**0.013**	**0.015**	**0.010**	**0.203**	**0.046**	**0.051**	**0.009**	**0.015**	**0.006**	**0.041**	**0.010**	**0.015**	**0.008**
MGDG(34:6)	0.000	0.000	0.001	0.001	0.000	0.000	0.000	0.000	0.001	0.001	0.000	0.000	0.000	0.000
MGDG(34:5)	0.000	0.000	0.001	0.001	0.000	0.000	0.001	0.001	0.000	0.000	0.000	0.000	0.000	0.000
MGDG(34:4)	0.000	0.000	0.000	0.000	0.000	0.000	0.000	0.000	0.000	0.000	0.000	0.000	0.001	0.000
MGDG(34:3)	0.001	0.001	0.001	0.000	0.004	0.001	0.001	0.001	0.002	0.001	0.001	0.000	0.002	0.001
MGDG(34:2)	0.003	0.002	0.001	0.001	0.002	0.001	0.001	0.000	0.001	0.000	0.000	0.000	0.001	0.001
MGDG(34:1)	0.000	0.000	0.000	0.000	0.000	0.000	0.000	0.000	0.000	0.000	0.000	0.000	0.000	0.000
MGDG(36:6)	0.006	0.003	0.005	0.004	0.031	0.000	0.014	0.006	0.007	0.005	0.007	0.002	0.007	0.003
MGDG(36:5)	0.021	0.011	0.018	0.017	0.067	0.011	0.011	0.002	0.008	0.003	0.021	0.007	0.005	0.003
MGDG(36:4)	0.063	0.032	0.006	0.004	0.050	0.010	0.009	0.001	0.007	0.003	0.017	0.006	0.003	0.002
MGDG(36:3)	0.001	0.000	0.001	0.001	0.003	0.002	0.003	0.000	0.002	0.001	0.003	0.001	0.001	0.001
MGDG(36:2)	0.000	0.000	0.000	0.000	0.000	0.000	0.001	0.001	0.000	0.000	0.001	0.000	0.000	0.000
MGDG(38:6)	0.001	0.001	0.000	0.000	0.000	0.000	0.000	0.000	0.000	0.000	0.000	0.000	0.000	0.000
MGDG(38:5)	0.001	0.001	0.003	0.002	0.000	0.000	0.000	0.000	0.002	0.001	0.000	0.000	0.000	0.000
MGDG(38:4)	0.000	0.000	0.011	0.010	0.000	0.000	0.000	0.000	0.003	0.003	0.000	0.000	0.000	0.000
MGDG(38:3)	0.000	0.000	0.001	0.001	0.000	0.000	0.000	0.000	0.000	0.000	0.000	0.000	0.000	0.001
Total MGDG	**0.099**	**0.052**	**0.050**	**0.041**	**0.158**	**0.022**	**0.042**	**0.007**	**0.032**	**0.012**	**0.050**	**0.016**	**0.021**	**0.010**

	Laurus nobilis		*Liriodendron tulipifera*		*Bambusa oldhamii*		*Triadica sebifera*		*Geijera parviflora*		*Distictis buccinatoria*		*Encelia farinosa*	
Compound*	**mean**	**std**	**mean**	**std**	**mean**	**std**	**mean**	**std**	**mean**	**std**	**mean**	**std**	**mean**	**std**
PG(32:0)	0.000	0.000	0.001	0.001	0.000	0.000	0.003	0.001	0.003	0.003	0.001	0.001	0.002	0.002
PG(34:4)	0.000	0.000	0.000	0.000	0.000	0.000	0.000	0.000	0.000	0.000	0.000	0.000	0.000	0.000
PG(34:3)	0.000	0.000	0.000	0.000	0.000	0.000	0.001	0.001	0.000	0.000	0.000	0.000	0.000	0.000
PG(34:2)	0.000	0.000	0.001	0.001	0.001	0.000	0.001	0.000	0.000	0.000	0.000	0.000	0.001	0.001
PG(34:1)	0.000	0.000	0.000	0.000	0.002	0.001	0.002	0.000	0.000	0.000	0.001	0.000	0.001	0.001
Total PG	**0.001**	**0.000**	**0.002**	**0.002**	**0.003**	**0.001**	**0.007**	**0.002**	**0.003**	**0.003**	**0.003**	**0.001**	**0.004**	**0.004**
LPG(16:1)	0.000	0.000	0.000	0.000	0.002	0.003	0.002	0.001	0.003	0.003	0.000	0.000	0.001	0.001
LPG(16:0)	0.008	0.002	0.006	0.003	0.012	0.004	0.006	0.002	0.004	0.003	0.004	0.001	0.006	0.001
LPG(18:3)	0.000	0.000	0.000	0.000	0.000	0.000	0.000	0.000	0.000	0.000	0.000	0.000	0.001	0.001
LPG(18:2)	0.001	0.000	0.001	0.001	0.004	0.003	0.000	0.000	0.001	0.000	0.001	0.001	0.001	0.000
LPG(18:1)	0.001	0.000	0.001	0.001	0.005	0.007	0.001	0.001	0.001	0.000	0.001	0.001	0.001	0.001
Total LysoPG	**0.010**	**0.002**	**0.008**	**0.003**	**0.024**	**0.013**	**0.010**	**0.004**	**0.008**	**0.006**	**0.005**	**0.003**	**0.010**	**0.003**
LPC(16:0)	0.000	0.000	0.001	0.001	0.000	0.000	0.001	0.001	0.001	0.001	0.001	0.000	0.003	0.002
LPC(18:3)	0.000	0.000	0.000	0.000	0.002	0.001	0.000	0.000	0.000	0.000	0.000	0.000	0.000	0.000
LPC(18:2)	0.000	0.000	0.001	0.001	0.005	0.002	0.001	0.001	0.000	0.000	0.000	0.000	0.002	0.001
LPC(18:1)	0.000	0.000	0.000	0.000	0.000	0.000	0.001	0.001	0.000	0.000	0.000	0.000	0.002	0.001
Total LysoPC	**0.000**	**0.000**	**0.003**	**0.003**	**0.006**	**0.003**	**0.004**	**0.002**	**0.001**	**0.001**	**0.001**	**0.001**	**0.007**	**0.004**
LPE(16:0)	0.001	0.001	0.000	0.000	0.001	0.000	0.001	0.001	0.001	0.001	0.001	0.000	0.003	0.003
LPE(18:3)	0.000	0.000	0.000	0.000	0.000	0.000	0.000	0.000	0.000	0.000	0.000	0.000	0.000	0.000
LPE(18:2)	0.000	0.000	0.000	0.000	0.002	0.002	0.000	0.001	0.000	0.000	0.000	0.000	0.001	0.001
LPE(18:1)	0.001	0.001	0.000	0.000	0.000	0.000	0.000	0.000	0.000	0.000	0.000	0.000	0.001	0.001
Total LysoPE	**0.002**	**0.002**	**0.001**	**0.001**	**0.003**	**0.002**	**0.002**	**0.002**	**0.001**	**0.001**	**0.001**	**0.001**	**0.005**	**0.005**
PC(32:0)	0.000	0.000	0.000	0.000	0.000	0.000	0.001	0.001	0.001	0.001	0.000	0.000	0.001	0.000
PC(34:4)	0.000	0.000	0.000	0.000	0.000	0.000	0.000	0.000	0.000	0.000	0.000	0.000	0.000	0.000
PC(34:3)	0.001	0.000	0.001	0.001	0.010	0.005	0.022	0.011	0.007	0.003	0.007	0.001	0.006	0.004
PC(34:2)	0.010	0.002	0.015	0.007	0.041	0.021	0.026	0.014	0.028	0.010	0.012	0.003	0.028	0.023
PC(34:1)	0.000	0.000	0.004	0.002	0.006	0.005	0.030	0.001	0.009	0.006	0.013	0.005	0.012	0.009
PC(36:6)	0.000	0.000	0.000	0.000	0.001	0.001	0.005	0.002	0.000	0.000	0.002	0.000	0.001	0.000
PC(36:5)	0.001	0.000	0.001	0.000	0.006	0.003	0.007	0.004	0.003	0.002	0.006	0.002	0.003	0.002
PC(36:4)	0.008	0.001	0.010	0.004	0.014	0.007	0.024	0.005	0.011	0.005	0.019	0.010	0.009	0.006
PC(36:3)	0.001	0.000	0.006	0.002	0.007	0.004	0.016	0.005	0.006	0.003	0.017	0.007	0.006	0.004

	Laurus nobilis		*Liriodendron tulipifera*		*Bambusa oldhamii*		*Triadica sebifera*		*Geijera parviflora*		*Distictis buccinatoria*		*Encelia farinosa*	
Compound*	**mean**	**std**	**mean**	**std**	**mean**	**std**	**mean**	**std**	**mean**	**std**	**mean**	**std**	**mean**	**std**
PC(36:2)	0.000	0.000	0.002	0.001	0.002	0.001	0.012	0.002	0.003	0.002	0.008	0.003	0.004	0.003
PC(36:1)	0.000	0.000	0.000	0.000	0.000	0.000	0.004	0.001	0.001	0.001	0.003	0.001	0.001	0.001
PC(38:6)	0.000	0.000	0.000	0.000	0.000	0.000	0.000	0.000	0.000	0.000	0.000	0.000	0.000	0.000
PC(38:5)	0.000	0.000	0.000	0.000	0.000	0.000	0.000	0.000	0.000	0.000	0.000	0.000	0.000	0.000
PC(38:4)	0.000	0.000	0.000	0.000	0.000	0.000	0.000	0.000	0.000	0.000	0.000	0.000	0.000	0.000
PC(38:3)	0.000	0.000	0.000	0.000	0.000	0.000	0.000	0.000	0.000	0.000	0.001	0.000	0.000	0.000
PC(38:2)	0.000	0.000	0.000	0.000	0.000	0.000	0.001	0.000	0.000	0.000	0.001	0.000	0.000	0.000
Total PC	**0.022**	**0.003**	**0.040**	**0.017**	**0.088**	**0.046**	**0.148**	**0.042**	**0.070**	**0.031**	**0.087**	**0.032**	**0.071**	**0.053**
PE(32:1)	0.000	0.000	0.000	0.000	0.000	0.000	0.000	0.000	0.000	0.000	0.000	0.000	0.000	0.001
PE(32:0)	0.000	0.000	0.000	0.000	0.000	0.000	0.000	0.000	0.000	0.000	0.000	0.000	0.000	0.000
PE(34:4)	0.000	0.000	0.000	0.000	0.000	0.000	0.000	0.000	0.000	0.000	0.000	0.000	0.000	0.000
PE(34:3)	0.000	0.000	0.000	0.000	0.003	0.002	0.008	0.008	0.005	0.001	0.004	0.001	0.004	0.004
PE(34:2)	0.003	0.000	0.008	0.006	0.013	0.010	0.012	0.012	0.030	0.010	0.012	0.005	0.024	0.028
PE(34:1)	0.000	0.000	0.001	0.001	0.000	0.000	0.006	0.005	0.003	0.002	0.005	0.002	0.004	0.006
PE(36:6)	0.000	0.000	0.000	0.000	0.000	0.000	0.002	0.002	0.000	0.000	0.001	0.000	0.000	0.000
PE(36:5)	0.000	0.000	0.000	0.000	0.001	0.001	0.002	0.002	0.001	0.000	0.003	0.001	0.001	0.002
PE(36:4)	0.003	0.001	0.003	0.002	0.006	0.005	0.005	0.005	0.007	0.003	0.009	0.004	0.005	0.006
PE(36:3)	0.000	0.000	0.001	0.001	0.001	0.001	0.003	0.003	0.002	0.001	0.007	0.003	0.002	0.003
PE(36:2)	0.000	0.000	0.001	0.001	0.000	0.000	0.002	0.002	0.001	0.001	0.004	0.002	0.002	0.003
PE(36:1)	0.000	0.000	0.000	0.000	0.000	0.000	0.001	0.001	0.000	0.000	0.001	0.000	0.000	0.000
PE(42:2)	0.000	0.000	0.000	0.000	0.000	0.000	0.000	0.000	0.001	0.000	0.000	0.000	0.001	0.001
Total PE	**0.007**	**0.001**	**0.016**	**0.014**	**0.026**	**0.020**	**0.042**	**0.042**	**0.051**	**0.016**	**0.046**	**0.018**	**0.046**	**0.055**
PI(32:2)	0.000	0.000	0.000	0.000	0.000	0.000	0.000	0.000	0.001	0.001	0.000	0.000	0.000	0.000
PI(32:1)	0.000	0.000	0.000	0.000	0.000	0.000	0.000	0.000	0.003	0.003	0.000	0.000	0.002	0.003
PI(32:0)	0.000	0.000	0.001	0.001	0.001	0.000	0.001	0.000	0.001	0.001	0.000	0.000	0.001	0.001
PI(34:4)	0.000	0.000	0.000	0.000	0.000	0.000	0.000	0.000	0.000	0.000	0.000	0.000	0.000	0.000
PI(34:3)	0.001	0.000	0.000	0.000	0.007	0.003	0.022	0.006	0.007	0.006	0.018	0.009	0.008	0.009
PI(34:2)	0.005	0.002	0.006	0.007	0.016	0.005	0.026	0.008	0.021	0.014	0.019	0.012	0.048	0.058
PI(34:1)	0.000	0.000	0.001	0.001	0.001	0.000	0.011	0.002	0.002	0.002	0.009	0.005	0.004	0.004
PI(36:6)	0.000	0.000	0.000	0.000	0.000	0.000	0.000	0.000	0.000	0.000	0.000	0.000	0.001	0.000
PI(36:5)	0.000	0.000	0.000	0.000	0.000	0.000	0.000	0.000	0.000	0.000	0.001	0.000	0.001	0.001
PI(36:4)	0.000	0.000	0.000	0.000	0.001	0.001	0.002	0.000	0.001	0.000	0.002	0.001	0.002	0.002

SUBMITTED MANUSCRIPT

	Laurus nobilis		*Liriodendron tulipifera*		*Bambusa oldhamii*		*Triadica sebifera*		*Geijera parviflora*		*Distictis buccinatoria*		*Encelia farinosa*	
Compound*	**mean**	**std**	**mean**	**std**	**mean**	**std**	**mean**	**std**	**mean**	**std**	**mean**	**std**	**mean**	**std**
PI(36:3)	0.000	0.000	0.000	0.000	0.001	0.000	0.002	0.001	0.000	0.000	0.001	0.001	0.001	0.001
PI(36:2)	0.000	0.000	0.000	0.000	0.000	0.000	0.002	0.000	0.001	0.001	0.001	0.001	0.002	0.002
PI(36:1)	0.000	0.000	0.000	0.000	0.000	0.000	0.001	0.000	0.000	0.000	0.000	0.000	0.000	0.000
Total PI	**0.007**	**0.003**	**0.009**	**0.009**	**0.027**	**0.009**	**0.068**	**0.018**	**0.035**	**0.027**	**0.051**	**0.030**	**0.071**	**0.081**
PS(34:3)	0.000	0.000	0.000	0.000	0.000	0.000	0.001	0.001	0.000	0.000	0.000	0.000	0.000	0.001
PS(34:2)	0.000	0.000	0.001	0.001	0.001	0.000	0.002	0.001	0.002	0.001	0.002	0.002	0.002	0.003
PS(34:1)	0.000	0.000	0.000	0.000	0.000	0.000	0.001	0.000	0.000	0.000	0.001	0.001	0.000	0.000
PS(36:6)	0.000	0.000	0.000	0.000	0.000	0.000	0.000	0.000	0.000	0.000	0.000	0.000	0.000	0.000
PS(36:5)	0.000	0.000	0.000	0.000	0.000	0.000	0.000	0.000	0.000	0.000	0.000	0.000	0.000	0.000
PS(36:4)	0.000	0.000	0.000	0.000	0.000	0.000	0.001	0.000	0.000	0.000	0.001	0.001	0.000	0.001
PS(36:3)	0.000	0.000	0.000	0.000	0.000	0.000	0.000	0.000	0.000	0.000	0.001	0.001	0.000	0.000
PS(36:2)	0.000	0.000	0.000	0.000	0.000	0.000	0.000	0.000	0.000	0.000	0.001	0.001	0.000	0.000
PS(38:3)	0.000	0.000	0.000	0.000	0.000	0.000	0.000	0.000	0.000	0.000	0.001	0.000	0.001	0.001
PS(38:2)	0.000	0.000	0.000	0.000	0.001	0.000	0.000	0.000	0.001	0.001	0.002	0.001	0.002	0.002
PS(38:1)	0.000	0.000	0.000	0.000	0.000	0.000	0.000	0.000	0.000	0.000	0.002	0.001	0.000	0.000
PS(40:3)	0.000	0.000	0.000	0.000	0.000	0.000	0.001	0.000	0.000	0.000	0.001	0.000	0.001	0.001
PS(40:2)	0.000	0.000	0.001	0.001	0.001	0.001	0.001	0.001	0.002	0.001	0.001	0.001	0.002	0.002
PS(40:1)	0.000	0.000	0.000	0.000	0.000	0.000	0.000	0.000	0.000	0.000	0.001	0.001	0.000	0.000
PS(42:4)	0.000	0.000	0.000	0.000	0.000	0.000	0.000	0.000	0.000	0.000	0.000	0.000	0.000	0.000
PS(42:3)	0.000	0.000	0.000	0.000	0.001	0.001	0.002	0.002	0.002	0.000	0.001	0.001	0.002	0.000
PS(42:2)	0.000	0.000	0.001	0.001	0.002	0.001	0.001	0.001	0.007	0.003	0.001	0.000	0.003	0.003
PS(44:3)	0.000	0.000	0.001	0.001	0.000	0.000	0.000	0.000	0.000	0.000	0.000	0.000	0.000	0.000
Total PS	**0.001**	**0.000**	**0.004**	**0.003**	**0.007**	**0.003**	**0.011**	**0.006**	**0.016**	**0.007**	**0.013**	**0.008**	**0.015**	**0.015**
PA(32:0)	0.000	0.000	0.000	0.000	0.001	0.001	0.001	0.001	0.003	0.002	0.001	0.001	0.002	0.001
PA(34:4)	0.000	0.000	0.000	0.000	0.000	0.000	0.000	0.000	0.000	0.000	0.000	0.000	0.001	0.000
PA(34:3)	0.000	0.000	0.002	0.001	0.014	0.006	0.023	0.012	0.029	0.017	0.018	0.010	0.029	0.014
PA(34:2)	0.002	0.001	0.021	0.016	0.045	0.020	0.024	0.014	0.115	0.065	0.029	0.015	0.113	0.059
PA(34:1)	0.000	0.000	0.004	0.003	0.009	0.004	0.023	0.003	0.020	0.011	0.022	0.012	0.029	0.019
PA(36:6)	0.000	0.000	0.000	0.000	0.000	0.000	0.004	0.003	0.001	0.000	0.002	0.001	0.003	0.002
PA(36:5)	0.000	0.000	0.001	0.001	0.008	0.003	0.007	0.004	0.009	0.006	0.011	0.006	0.015	0.008
PA(36:4)	0.001	0.001	0.007	0.005	0.024	0.011	0.014	0.003	0.026	0.014	0.025	0.016	0.033	0.019
PA(36:3)	0.000	0.000	0.004	0.002	0.007	0.002	0.011	0.004	0.012	0.005	0.027	0.018	0.021	0.014

	Laurus nobilis		*Liriodendron tulipifera*		*Bambusa oldhamii*		*Triadica sebifera*		*Geijera parviflora*		*Distictis buccinatoria*		*Encelia farinosa*	
Compound*	**mean**	**std**	**mean**	**std**	**mean**	**std**	**mean**	**std**	**mean**	**std**	**mean**	**std**	**mean**	**std**
PA(36:2)	0.000	0.000	0.002	0.001	0.003	0.002	0.012	0.002	0.008	0.004	0.017	0.010	0.016	0.010
Total PA	**0.004**	**0.002**	**0.041**	**0.030**	**0.112**	**0.049**	**0.120**	**0.047**	**0.223**	**0.125**	**0.153**	**0.090**	**0.262**	**0.144**
SQDG(34:3)	n.d.		0.000	0.000	n.d.		0.001	0.001	0.000	0.000	0.001	0.000	0.001	0.000
SQDG(34:2)	n.d.		0.000	0.000	n.d.		0.001	0.000	0.001	0.002	0.001	0.000	0.004	0.002
SQDG(34:1)	n.d.		0.000	0.000	n.d.		0.001	0.000	0.000	0.000	0.001	0.000	0.001	0.000
SQDG(36:5)	n.d.		0.000	0.000	n.d.		0.000	0.000	0.000	0.000	0.000	0.000	0.001	0.001
SQDG(36:4)	n.d.		0.000	0.000	n.d.		0.000	0.000	0.000	0.000	0.000	0.000	0.001	0.000
Total SQDG	n.d.		**0.001**	**0.001**	n.d.		**0.003**	**0.000**	**0.003**	**0.001**	**0.003**	**0.001**	**0.009**	**0.003**

* DGDG = digalactosyldiacylglycerol; LPC = lysophosphatidylcholine; LPE = lysophosphatidylethanolamine; LPG = lysophosphatidylglycerol; MGDG = monogalactosyldiacylglycerol; PA = phosphatidic acid; PC = phosphatidylcholine; PE = phosphatidylethanolamine; PG = phosphatidylglycerol; PI = phosphatidylinositol; PS = phosphatidylserine

Table S3. Lipids in cell contamination controls for xylem sap (mean of n = 4, µmol L^{-1}). In parentheses: Number of carbon atoms in acyl chain:number of double bonds.

	Laurus nobilis		*Liriodendron tulipifera*		*Bambusa oldhamii*		*Triadica sebifera*		*Geijera parviflora*		*Distictis buccinatoria*		*Encelia farinosa*	
Compound*	**mean**	**std**	**mean**	**std**	**mean**	**std**	**mean**	**std**	**mean**	**std**	**mean**	**std**	**mean**	**std**
DGDG((34:4)	0.000	0.000	0.000	0.000	0.000	0.000	0.000	0.000	0.000	0.000	0.000	0.000	0.000	0.000
DGDG((34:3)	0.000	0.000	0.000	0.000	0.001	0.001	0.000	0.000	0.000	0.000	0.000	0.000	0.000	0.000
DGDG((34:2)	0.000	0.000	0.000	0.000	0.001	0.001	0.000	0.000	0.000	0.000	0.000	0.000	0.000	0.000
DGDG((34:1)	0.000	0.000	0.000	0.000	0.000	0.000	0.000	0.000	0.000	0.000	0.000	0.000	0.000	0.000
DGDG((36:6)	0.000	0.000	0.000	0.000	0.000	0.000	0.000	0.000	0.000	0.000	0.000	0.000	0.000	0.000
DGDG((36:5)	0.001	0.000	0.000	0.001	0.001	0.001	0.000	0.000	0.000	0.000	0.000	0.000	0.000	0.000
DGDG((36:4)	0.001	0.000	0.001	0.001	0.001	0.001	0.000	0.000	0.000	0.000	0.000	0.000	0.000	0.000
DGDG((36:3)	0.000	0.000	0.001	0.002	0.000	0.000	0.000	0.000	0.000	0.000	0.000	0.000	0.000	0.000
DGDG((36:2)	0.000	0.000	0.000	0.000	0.000	0.000	0.000	0.000	0.000	0.000	0.000	0.000	0.000	0.000
DGDG((36:1)	0.000	0.000	0.000	0.000	0.000	0.000	0.000	0.000	0.000	0.000	0.000	0.000	0.000	0.000
DGDG((38:6)	0.000	0.000	0.000	0.000	0.000	0.000	0.000	0.000	0.000	0.000	0.000	0.000	0.000	0.000
DGDG((38:5)	0.000	0.000	0.000	0.000	0.000	0.000	0.000	0.000	0.000	0.000	0.000	0.000	0.000	0.000
DGDG((38:4)	0.000	0.000	0.001	0.001	0.000	0.000	0.000	0.000	0.000	0.000	0.000	0.000	0.000	0.000
Total DGDG	**0.003**	**0.001**	**0.005**	**0.007**	**0.005**	**0.004**	**0.001**	**0.001**	**0.001**	**0.002**	**0.002**	**0.001**	**0.000**	**0.000**
MGDG((34:6)	0.000	0.000	0.000	0.000	0.000	0.000	0.000	0.000	0.000	0.000	0.000	0.000	0.000	0.000
MGDG((34:5)	0.000	0.000	0.002	0.003	0.000	0.000	0.000	0.000	0.000	0.000	0.000	0.000	0.000	0.000
MGDG((34:4)	0.000	0.000	0.000	0.000	0.000	0.000	0.000	0.000	0.000	0.000	0.000	0.000	0.000	0.000
MGDG((34:3)	0.000	0.000	0.000	0.000	0.000	0.000	0.000	0.000	0.000	0.000	0.000	0.000	0.000	0.000
MGDG((34:2)	0.000	0.000	0.000	0.000	0.000	0.000	0.000	0.000	0.000	0.000	0.000	0.000	0.000	0.000
MGDG((34:1)	0.000	0.000	0.000	0.000	0.000	0.000	0.000	0.000	0.000	0.000	0.000	0.000	0.000	0.000
MGDG((36:6)	0.001	0.000	0.000	0.001	0.002	0.001	0.001	0.000	0.001	0.000	0.000	0.000	0.000	0.000
MGDG((36:5)	0.001	0.000	0.001	0.000	0.004	0.004	0.000	0.000	0.000	0.000	0.001	0.001	0.000	0.000
MGDG((36:4)	0.002	0.000	0.000	0.000	0.003	0.003	0.000	0.000	0.000	0.000	0.001	0.001	0.000	0.000
MGDG((36:3)	0.000	0.000	0.000	0.000	0.000	0.000	0.000	0.000	0.000	0.000	0.000	0.000	0.000	0.000
MGDG((36:2)	0.000	0.000	0.000	0.000	0.000	0.000	0.000	0.000	0.000	0.000	0.000	0.000	0.000	0.000
MGDG((38:6)	0.000	0.000	0.000	0.000	0.000	0.000	0.000	0.000	0.000	0.000	0.000	0.000	0.000	0.000
MGDG((38:5)	0.000	0.000	0.000	0.000	0.000	0.000	0.000	0.000	0.000	0.000	0.000	0.000	0.000	0.000
MGDG((38:4)	0.000	0.000	0.000	0.000	0.000	0.000	0.000	0.000	0.000	0.000	0.000	0.000	0.000	0.000
MGDG((38:3)	0.000	0.000	0.000	0.000	0.000	0.000	0.000	0.000	0.000	0.000	0.000	0.000	0.000	0.000
Total MGDG	**0.004**	**0.002**	**0.004**	**0.004**	**0.010**	**0.009**	**0.001**	**0.000**	**0.002**	**0.001**	**0.002**	**0.001**	**0.001**	**0.000**

	Laurus nobilis		*Liriodendron tulipifera*		*Bambusa oldhamii*		*Triadica sebifera*		*Geijera parviflora*		*Distictis buccinatoria*		*Encelia farinosa*	
Compound*	**mean**	**std**	**mean**	**std**	**mean**	**std**	**mean**	**std**	**mean**	**std**	**mean**	**std**	**mean**	**std**
PG((32:0)	0.000	0.000	0.000	0.000	0.000	0.000	0.000	0.000	0.000	0.000	0.000	0.000	0.000	0.000
PG((34:4)	0.000	0.000	0.000	0.000	0.000	0.000	0.000	0.000	0.000	0.000	0.000	0.000	0.000	0.000
PG((34:3)	0.000	0.000	0.000	0.000	0.000	0.000	0.000	0.000	0.000	0.000	0.000	0.000	0.000	0.000
PG((34:2)	0.000	0.000	0.000	0.000	0.000	0.000	0.000	0.000	0.000	0.000	0.000	0.000	0.000	0.000
PG((34:1)	0.000	0.000	0.000	0.000	0.000	0.000	0.000	0.000	0.000	0.000	0.000	0.000	0.000	0.000
Total PG	**0.000**	**0.000**	**0.000**	**0.000**	**0.000**	**0.001**	**0.000**	**0.000**	**0.000**	**0.000**	**0.000**	**0.000**	**0.000**	**0.000**
LPG((16:1)	0.000	0.000	0.000	0.000	0.000	0.000	0.000	0.000	0.001	0.000	0.000	0.000	0.000	0.000
LPG((16:0)	0.005	0.001	0.003	0.003	0.008	0.001	0.002	0.001	0.003	0.001	0.003	0.001	0.002	0.000
LPG((18:3)	0.000	0.000	0.000	0.000	0.000	0.000	0.000	0.000	0.000	0.000	0.000	0.000	0.000	0.000
LPG((18:2)	0.001	0.000	0.000	0.000	0.000	0.000	0.000	0.000	0.000	0.000	0.000	0.000	0.000	0.000
LPG((18:1)	0.001	0.001	0.001	0.000	0.000	0.000	0.000	0.000	0.000	0.000	0.000	0.000	0.000	0.000
Total LysoPG	**0.006**	**0.002**	**0.004**	**0.002**	**0.008**	**0.001**	**0.002**	**0.001**	**0.004**	**0.001**	**0.003**	**0.002**	**0.002**	**0.000**
LPC((16:0)	0.000	0.000	0.000	0.000	0.000	0.000	0.000	0.000	0.000	0.000	0.000	0.000	0.000	0.000
LPC((18:3)	0.000	0.000	0.000	0.000	0.000	0.000	0.000	0.000	0.000	0.000	0.000	0.000	0.000	0.000
LPC((18:2)	0.000	0.000	0.000	0.000	0.000	0.000	0.000	0.000	0.000	0.000	0.000	0.000	0.000	0.000
LPC((18:1)	0.000	0.000	0.000	0.000	0.000	0.000	0.000	0.000	0.000	0.000	0.000	0.000	0.000	0.000
Total LysoPC	**0.000**	**0.000**	**0.000**	**0.000**	**0.001**	**0.000**	**0.000**	**0.000**	**0.000**	**0.000**	**0.000**	**0.000**	**0.000**	**0.000**
LPE((16:0)	0.002	0.001	0.000	0.000	0.001	0.001	0.000	0.000	0.000	0.000	0.000	0.000	0.000	0.000
LPE((18:3)	0.000	0.000	0.000	0.000	0.000	0.000	0.000	0.000	0.000	0.000	0.000	0.000	0.000	0.000
LPE((18:2)	0.000	0.000	0.000	0.000	0.000	0.000	0.000	0.000	0.000	0.000	0.000	0.000	0.000	0.000
LPE((18:1)	0.000	0.001	0.000	0.000	0.000	0.000	0.000	0.000	0.000	0.000	0.000	0.000	0.000	0.000
Total LysoPE	**0.003**	**0.002**	**0.000**	**0.000**	**0.001**	**0.001**	**0.000**	**0.000**	**0.000**	**0.000**	**0.000**	**0.000**	**0.000**	**0.000**
PC((32:0)	0.000	0.000	0.000	0.000	0.000	0.000	0.000	0.000	0.000	0.000	0.000	0.000	0.000	0.000
PC((34:4)	0.000	0.000	0.000	0.000	0.000	0.000	0.000	0.000	0.000	0.000	0.000	0.000	0.000	0.000
PC((34:3)	0.000	0.000	0.000	0.000	0.001	0.002	0.001	0.001	0.001	0.000	0.000	0.000	0.001	0.000
PC((34:2)	0.001	0.001	0.001	0.000	0.004	0.006	0.001	0.000	0.002	0.000	0.000	0.000	0.004	0.000
PC((34:1)	0.000	0.000	0.000	0.000	0.001	0.001	0.002	0.001	0.001	0.000	0.001	0.000	0.001	0.000
PC((36:6)	0.000	0.000	0.000	0.000	0.000	0.000	0.000	0.000	0.000	0.000	0.000	0.000	0.000	0.000
PC((36:5)	0.000	0.000	0.000	0.000	0.001	0.001	0.000	0.000	0.000	0.000	0.000	0.000	0.001	0.000
PC((36:4)	0.000	0.001	0.001	0.000	0.001	0.002	0.002	0.001	0.001	0.001	0.001	0.000	0.003	0.002
PC((36:3)	0.000	0.000	0.001	0.000	0.001	0.001	0.001	0.001	0.001	0.000	0.001	0.000	0.001	0.000

Compound*	*Laurus nobilis* mean	*Laurus nobilis* std	*Liriodendron tulipifera* mean	*Liriodendron tulipifera* std	*Bambusa oldhamii* mean	*Bambusa oldhamii* std	*Triadica sebifera* mean	*Triadica sebifera* std	*Geijera parviflora* mean	*Geijera parviflora* std	*Distictis buccinatoria* mean	*Distictis buccinatoria* std	*Encelia farinosa* mean	*Encelia farinosa* std
PC((36:2)	0.000	0.000	0.000	0.000	0.000	0.000	0.001	0.000	0.000	0.000	0.000	0.000	0.001	0.000
PC((36:1)	0.000	0.000	0.000	0.000	0.000	0.000	0.000	0.000	0.000	0.000	0.000	0.000	0.000	0.000
PC((38:6)	0.000	0.000	0.000	0.000	0.000	0.000	0.000	0.000	0.000	0.000	0.000	0.000	0.000	0.000
PC((38:5)	0.000	0.000	0.000	0.000	0.000	0.000	0.000	0.000	0.000	0.000	0.000	0.000	0.000	0.000
PC((38:4)	0.000	0.000	0.000	0.000	0.000	0.000	0.000	0.000	0.000	0.000	0.000	0.000	0.000	0.000
PC((38:3)	0.000	0.000	0.000	0.000	0.000	0.000	0.000	0.000	0.000	0.000	0.000	0.000	0.000	0.000
PC((38:2)	0.000	0.000	0.000	0.000	0.000	0.000	0.000	0.000	0.000	0.000	0.000	0.000	0.000	0.000
Total PC	**0.002**	**0.002**	**0.003**	**0.001**	**0.008**	**0.013**	**0.008**	**0.005**	**0.007**	**0.001**	**0.003**	**0.000**	**0.012**	**0.004**
PE((32:1)	0.000	0.000	0.000	0.000	0.000	0.000	0.000	0.000	0.000	0.000	0.000	0.000	0.000	0.000
PE((32:0)	0.000	0.000	0.000	0.000	0.000	0.000	0.000	0.000	0.000	0.000	0.000	0.000	0.000	0.000
PE((34:4)	0.000	0.000	0.000	0.000	0.000	0.000	0.000	0.000	0.000	0.000	0.000	0.000	0.000	0.000
PE((34:3)	0.000	0.000	0.000	0.000	0.000	0.000	0.000	0.000	0.000	0.000	0.000	0.000	0.000	0.000
PE((34:2)	0.000	0.000	0.000	0.000	0.000	0.000	0.000	0.001	0.000	0.000	0.000	0.000	0.000	0.000
PE((34:1)	0.000	0.000	0.000	0.000	0.000	0.000	0.000	0.000	0.000	0.000	0.000	0.000	0.000	0.000
PE((36:6)	0.000	0.000	0.000	0.000	0.000	0.000	0.000	0.000	0.000	0.000	0.000	0.000	0.000	0.000
PE((36:5)	0.000	0.000	0.000	0.000	0.000	0.000	0.000	0.000	0.000	0.000	0.000	0.000	0.000	0.000
PE((36:4)	0.000	0.000	0.000	0.000	0.000	0.000	0.000	0.000	0.000	0.000	0.000	0.000	0.000	0.000
PE((36:3)	0.000	0.000	0.000	0.000	0.000	0.000	0.000	0.000	0.000	0.000	0.000	0.000	0.000	0.000
PE((36:2)	0.000	0.000	0.000	0.000	0.000	0.000	0.000	0.000	0.000	0.000	0.000	0.000	0.000	0.000
PE((36:1)	0.000	0.000	0.000	0.000	0.000	0.000	0.000	0.000	0.000	0.000	0.000	0.000	0.000	0.000
PE((42:2)	0.000	0.000	0.000	0.000	0.000	0.000	0.000	0.000	0.000	0.000	0.000	0.000	0.000	0.000
Total PE	**0.000**	**0.000**	**0.000**	**0.000**	**0.000**	**0.000**	**0.002**	**0.002**	**0.000**	**0.000**	**0.000**	**0.000**	**0.000**	**0.000**
PI((32:2)	0.000	0.000	0.000	0.000	0.000	0.000	0.000	0.000	0.000	0.000	0.000	0.000	0.000	0.000
PI((32:1)	0.000	0.000	0.000	0.000	0.000	0.000	0.000	0.000	0.000	0.000	0.000	0.000	0.000	0.000
PI((32:0)	0.000	0.000	0.000	0.000	0.000	0.000	0.000	0.000	0.000	0.000	0.000	0.000	0.000	0.000
PI((34:4)	0.000	0.000	0.000	0.000	0.000	0.000	0.000	0.000	0.000	0.000	0.000	0.000	0.000	0.000
PI((34:3)	0.000	0.000	0.000	0.000	0.000	0.000	0.000	0.001	0.000	0.000	0.000	0.000	0.000	0.000
PI((34:2)	0.000	0.001	0.000	0.000	0.000	0.001	0.001	0.001	0.000	0.000	0.000	0.000	0.000	0.000
PI((34:1)	0.000	0.000	0.000	0.000	0.000	0.000	0.000	0.001	0.000	0.000	0.000	0.000	0.000	0.000
PI((36:6)	0.000	0.000	0.000	0.000	0.000	0.000	0.000	0.000	0.000	0.000	0.000	0.000	0.000	0.000
PI((36:5)	0.000	0.000	0.000	0.000	0.000	0.000	0.000	0.000	0.000	0.000	0.000	0.000	0.000	0.000
PI((36:4)	0.000	0.000	0.000	0.000	0.000	0.000	0.000	0.000	0.000	0.000	0.000	0.000	0.000	0.000

	Laurus nobilis		*Liriodendron tulipifera*		*Bambusa oldhamii*		*Triadica sebifera*		*Geijera parviflora*		*Distictis buccinatoria*		*Encelia farinosa*	
Compound*	**mean**	**std**	**mean**	**std**	**mean**	**std**	**mean**	**std**	**mean**	**std**	**mean**	**std**	**mean**	**std**
PI((36:3)	0.000	0.000	0.000	0.000	0.000	0.000	0.000	0.000	0.000	0.000	0.000	0.000	0.000	0.000
PI((36:2)	0.000	0.000	0.000	0.000	0.000	0.000	0.000	0.000	0.000	0.000	0.000	0.000	0.000	0.000
PI((36:1)	0.000	0.000	0.000	0.000	0.000	0.000	0.000	0.000	0.000	0.000	0.000	0.000	0.000	0.000
Total PI	**0.001**	**0.001**	**0.000**	**0.000**	**0.001**	**0.001**	**0.002**	**0.003**	**0.000**	**0.000**	**0.000**	**0.000**	**0.000**	**0.000**
PS((34:3)	0.000	0.000	0.000	0.000	0.000	0.000	0.000	0.000	0.000	0.000	0.000	0.000	0.000	0.000
PS((34:2)	0.000	0.000	0.000	0.000	0.000	0.000	0.000	0.000	0.000	0.000	0.000	0.000	0.000	0.000
PS((34:1)	0.000	0.000	0.000	0.000	0.000	0.000	0.000	0.000	0.000	0.000	0.000	0.000	0.000	0.000
PS((36:6)	0.000	0.000	0.000	0.000	0.000	0.000	0.000	0.000	0.000	0.000	0.000	0.000	0.000	0.000
PS((36:5)	0.000	0.000	0.000	0.000	0.000	0.000	0.000	0.000	0.000	0.000	0.000	0.000	0.000	0.000
PS((36:4)	0.000	0.000	0.000	0.000	0.000	0.000	0.000	0.000	0.000	0.000	0.000	0.000	0.000	0.000
PS((36:3)	0.000	0.000	0.000	0.000	0.000	0.000	0.000	0.000	0.000	0.000	0.000	0.000	0.000	0.000
PS((36:2)	0.000	0.000	0.000	0.000	0.000	0.000	0.000	0.000	0.000	0.000	0.000	0.000	0.000	0.000
PS((38:3)	0.000	0.000	0.000	0.000	0.000	0.000	0.000	0.000	0.000	0.000	0.000	0.000	0.000	0.000
PS((38:2)	0.000	0.000	0.000	0.000	0.000	0.000	0.000	0.000	0.000	0.000	0.000	0.000	0.000	0.000
PS((38:1)	0.000	0.001	0.000	0.000	0.000	0.000	0.000	0.000	0.000	0.000	0.000	0.000	0.000	0.000
PS((40:3)	0.000	0.000	0.000	0.000	0.000	0.000	0.000	0.000	0.000	0.000	0.000	0.000	0.000	0.000
PS((40:2)	0.000	0.000	0.000	0.000	0.000	0.000	0.000	0.000	0.000	0.000	0.000	0.000	0.000	0.000
PS((40:1)	0.000	0.000	0.000	0.000	0.000	0.000	0.000	0.000	0.000	0.000	0.000	0.000	0.000	0.000
PS((42:4)	0.000	0.000	0.000	0.000	0.000	0.000	0.000	0.000	0.000	0.000	0.000	0.000	0.000	0.000
PS((42:3)	0.000	0.000	0.000	0.000	0.000	0.000	0.000	0.000	0.000	0.000	0.000	0.000	0.000	0.000
PS((42:2)	0.000	0.000	0.000	0.000	0.000	0.000	0.000	0.000	0.000	0.000	0.000	0.000	0.000	0.000
PS((44:3)	0.000	0.000	0.000	0.000	0.000	0.000	0.000	0.000	0.000	0.000	0.000	0.000	0.000	0.000
Total PS	**0.001**	**0.001**	**0.000**	**0.000**	**0.000**	**0.000**	**0.000**	**0.000**	**0.000**	**0.000**	**0.000**	**0.001**	**0.000**	**0.000**
PA((32:0)	0.000	0.000	0.000	0.000	0.000	0.000	0.000	0.000	0.000	0.000	0.000	0.000	0.000	0.000
PA((34:4)	0.000	0.000	0.000	0.000	0.000	0.000	0.000	0.000	0.000	0.000	0.000	0.000	0.000	0.000
PA((34:3)	0.000	0.000	0.000	0.000	0.000	0.000	0.002	0.001	0.002	0.001	0.000	0.000	0.001	0.000
PA((34:2)	0.000	0.000	0.002	0.001	0.001	0.001	0.002	0.001	0.003	0.002	0.000	0.000	0.003	0.001
PA((34:1)	0.000	0.000	0.001	0.001	0.000	0.000	0.002	0.002	0.001	0.001	0.000	0.000	0.001	0.000
PA((36:6)	0.000	0.000	0.000	0.000	0.000	0.000	0.000	0.000	0.000	0.000	0.000	0.000	0.000	0.000
PA((36:5)	0.000	0.000	0.000	0.000	0.000	0.000	0.000	0.000	0.001	0.001	0.000	0.000	0.001	0.000
PA((36:4)	0.000	0.000	0.002	0.001	0.000	0.000	0.002	0.001	0.001	0.001	0.000	0.000	0.001	0.000
PA((36:3)	0.000	0.000	0.001	0.000	0.000	0.000	0.001	0.001	0.001	0.001	0.000	0.000	0.001	0.000

Compound*	*Laurus nobilis* mean	*Laurus nobilis* std	*Liriodendron tulipifera* mean	*Liriodendron tulipifera* std	*Bambusa oldhamii* mean	*Bambusa oldhamii* std	*Triadica sebifera* mean	*Triadica sebifera* std	*Geijera parviflora* mean	*Geijera parviflora* std	*Distictis buccinatoria* mean	*Distictis buccinatoria* std	*Encelia farinosa* mean	*Encelia farinosa* std
PA((36:2)	0.000	0.000	0.001	0.000	0.000	0.000	0.001	0.001	0.000	0.000	0.000	0.000	0.000	0.000
Total PA	**0.000**	**0.000**	**0.007**	**0.004**	**0.002**	**0.002**	**0.011**	**0.006**	**0.009**	**0.006**	**0.002**	**0.000**	**0.006**	**0.001**
SQDG((34:3)			0.000	0.000			0.000	0.000	0.000	0.000	0.000	0.000	0.000	0.000
SQDG((34:2)			0.000	0.000			0.000	0.000	0.000	0.000	0.000	0.000	0.000	0.000
SQDG((34:1)			0.000	0.000			0.000	0.000	0.000	0.000	0.000	0.000	0.000	0.000
SQDG((36:5)			0.000	0.000			0.000	0.000	0.000	0.000	0.000	0.000	0.000	0.000
SQDG((36:4)			0.000	0.000			0.000	0.000	0.000	0.000	0.000	0.000	0.000	0.000
Total SQDG			**0.001**	**0.001**			**0.003**	**0.000**	**0.003**	**0.001**	**0.003**	**0.001**	**0.009**	**0.003**

* DGDG = digalactosyldiacylglycerol; LPC = lysophosphatidylcholine; LPE = lysophosphatidylethanolamine; LPG = lysophosphatidylglycerol; MGDG = monogalactosyldiacylglycerol; PA = phosphatidic acid; PC = phosphatidylcholine; PE = phosphatidylethanolamine; PG = phosphatidylglycerol; PI = phosphatidylinositol; PS = phosphatidylserine